

Preprint Numbers: KSUCNR-02-96  
 TRI-PP-96-25  
 nucl-th/9607025

## Pion Loop Contribution to $\rho - \omega$ Mixing and Mass Splitting

K. L. Mitchell\* and P. C. Tandy

*Center for Nuclear Research, Department of Physics, Kent State University, Kent, Ohio 44242*  
 (July 12, 1996)

### Abstract

We study the self-energy amplitudes for the  $\rho - \omega$  meson system produced by an effective field theory model at the quark level characterized by a finite range quark-quark interaction and an isospin breaking bare quark mass difference  $m_u - m_d$ . Dynamical effects associated with confinement and dressing of quarks and the finite size of the produced  $\bar{q}q$  meson modes are treated. Parameters of this approach, previously constrained by soft pion physics, are here supplemented in a minimal way to reproduce  $m_\omega$  and  $g_{\rho\pi\pi}$ . Calculations are carried out up to the one pion loop level and the predictions for  $\rho^0 - \omega$  mixing, mass splitting, the  $\rho$  width and the symmetry breaking  $\omega\pi\pi$  coupling constant and form factor are presented. The contribution of the direct  $\omega \rightarrow \pi\pi$  process relative to the  $\omega \rightarrow \rho \rightarrow \pi\pi$  process is discussed within this model.

PACS numbers: 24.85.+p, 12.40.Yx, 12.39.Ki, 13.75.Lb

## I. INTRODUCTION

Recent work on the pion and kaon systems has shown [1,2] that a very efficient description of masses, decay constants and electromagnetic form factors in terms of QCD degrees of freedom can be implemented through a parameterized form of the dressed quark propagator used in conjunction with truncations of the coupled Dyson-Schwinger equations (DSE). Chiral symmetry considerations for these systems eliminate the need for explicit information about gluon propagators and the gluon-quark vertex apart from that which is implicitly provided by the dressed quark propagator. At the simplest level this DSE approach [3] to the QCD modeling of hadron physics has been successful in a number of applications involving the Goldstone bosons including  $\pi\pi$  scattering [4] and the anomalous  $\gamma^*\pi\gamma$  [5],  $\gamma\pi\pi\pi$  [6] and  $\gamma\pi\rho$  [7,8] processes. The dynamical format of these initial studies can also be generated from a model field theory with QCD degrees of freedom containing an effective finite range gluon propagator. In particular, a treatment at the  $0^{th}$  order in the loop expansion of the produced  $\bar{q}q$  Goldstone meson modes will yield the same dynamical structure with a consistently specified content for the various dressed elements. We take this latter point of view for the present work and consider a minimal extension beyond the Goldstone boson sector to address some interesting issues in the  $\rho - \omega$  vector meson system. A previous work on  $\rho - \omega$  mixing with this approach, [9] limited to  $0^{th}$  order in meson loops, is here extended to the one pion loop level to address a wider set of phenomena.

Quark confinement should be an important element in the bound state dynamics and hadronic decays of the  $\rho - \omega$  system. Otherwise, with typical constituent  $u$  and  $d$  quark masses of about 350 MeV, the nearby spurious  $\bar{q}q$  production threshold would have undue influence. The approach we take incorporates quark confinement through the absence of a mass-shell pole in the employed dressed quark propagator. The necessary momentum dependence of the quark self-energy amplitudes implies a finite range for the effective gluon propagator. The associated quark momentum dependence of the meson-quark vertex functions reflects the finite size of the  $\bar{q}q$  correlations. To guide our development of an effective action for  $\pi$ ,  $\rho$  and  $\omega$  that preserves these realistic features we use the two flavor version of the Global Color Model (GCM) [10,11]. The employed dressed quark propagator model is constrained by soft chiral physics and is a simplified version of what is currently available [1,2] in order to facilitate the type of calculations necessary for this work. Information about the dressed gluon propagator, necessary to treat mesons that are not Goldstone mesons, is here introduced in a minimal way that is constrained by calculated values of  $m_\omega$  and  $g_{\rho\pi\pi}$ .

The zero range limit of the model we employ is very closely related to the Nambu–Jona-Lasinio model (NJL) [12] which has been extensively used to model hadron physics. However, in contrast with the present approach based upon the GCM, many important loop integrals encountered within the NJL model must be regulated via additional parameters. Also quark confinement cannot be generated from the contact NJL interaction and the dynamically generated quark mass is a constant (constituent mass) rather than the (running) mass function which is a necessary consequence of finite range gluon propagation. The associated nonlocalities have a profound effect upon the nature of the calculations and the role that is assigned to phenomenology. A previous study of the  $\rho - \omega$  system within the NJL model was limited to the quark loop level for the mixing amplitude, but did generate the  $\rho$  propagator, including the  $2\pi$  width, at the pion loop level [13]. In Refs. [14,15] an

extended NJL model that includes an extra confining interaction has been applied to the  $\rho - \omega$  system in a way that is the most comparable to the approach we take.

One of the topics we investigate is  $\rho^0 - \omega$  mixing generated by the bare quark mass difference  $m_d - m_u$ . Recent interest in a description of  $\rho^0 - \omega$  mixing from the quark level has centered around the momentum dependence of the mixed self-energy amplitude and the possible contribution to the charge symmetry breaking (CSB) component of the nucleon-nucleon force. [9,16,17] The quark loop mechanism produces a momentum dependence that suppresses the amplitude at the small space-like momenta appropriate to the mixed  $\rho - \omega$  exchange mechanism. Here we investigate the one pion loop correction and find that the space-like mixing still remains negligibly small. A more promising explanation for the CSB nuclear force has been found in the meson-nucleon vertex [18].

Our study of the pion loop contributions to the self-energies of the  $\rho - \omega$  system produces calculations of the  $\rho\pi\pi$  and  $\omega\pi\pi$  coupling constants and form factors as well as the  $2\pi$  width of the  $\rho$  and the mass splitting  $m_\rho - m_\omega$ . Initial studies within the GCM of  $m_\rho - m_\omega$  [19] and  $g_{\rho\pi\pi}$  [20] approximated hadron mass-shell information by behavior at zero meson momenta. This was to avoid ambiguities associated with numerical extrapolations of dressed quark propagators to the complex momenta needed to put hadron momenta on-shell in this Euclidean space approach. The correct mass-shell definitions can be maintained in the present work due to the assured analytic properties of the model quark propagator employed.

The amplitude for the direct process  $\omega_I \rightarrow \pi \pi$  is conventionally assumed [21] to cancel out in the analysis of  $e^+ e^- \rightarrow \pi \pi$  data to extract a value for the physical  $\rho^0 - \omega$  mixing amplitude [22]. Here  $\omega_I$  is the pure isospin component of the physical  $\rho$ . However, it has recently been argued [23] that, without a theoretical model for the  $\omega_I \rightarrow \pi \pi$  amplitude, the error on the extracted mixing amplitude is much greater than previously thought. Evidence for a significant contribution from the  $\omega_I\pi\pi$  process is obtained in a recent QCD sum rule analysis of the mixed-isospin vector current correlator [24]. In contrast, the value for  $g_{\omega_I\pi\pi}$  recently estimated from the extended NJL model of Ref. [15] suggests a negligible effect. In the present work, the strength of this G-parity violating  $\omega_I\pi\pi$  coupling, as driven by  $m_d - m_u$  in the underlying quark loop, is found to be significant enough to require an increase of typically 20% in the required mixing amplitude.

In Sec. II we describe the underlying quark model action and also general aspects of the resulting effective meson action that we shall use. The connection between them, i.e. the generation of  $\bar{q}q$  meson modes from the GCM action, has been covered in previous works and key elements are here reviewed briefly in the Appendix. Specific aspects of the pion sector, and the model dressed quark propagator which is constrained by it, are described in Sec. III. The mixed  $\rho - \omega$  meson sector produced at tree level by integrating out the quarks is described in detail in Sec. IV. At that same level, the produced  $\rho\pi\pi$  and  $\omega\pi\pi$  interactions are identified in Sec. V and the calculated coupling constants and form factors are described. The pions are integrated out up to the one loop level in Sec. VI and the contributions to the mixing as well as to the  $\rho$  width and mass shift are described. Also presented in Sec. VI is a discussion of the relative contribution of  $\rho^0 - \omega$  mixing and the direct process  $\omega_I \rightarrow \pi \pi$  to the physical coupling strength  $g_{\omega\pi\pi}$ . Further discussion follows in Sec. VII.

## II. QUARK MODEL

To obtain a practical covariant description of both meson substructure and interactions in terms of dynamically dressed quark degrees of freedom we use the Global Color Model [10,11]. This is an effective field theory at the quark level described by the action

$$S[\bar{q}, q] = \int d^4x \bar{q}(x)(\gamma \cdot \partial_x + m)q(x) + \frac{1}{2} \int d^4x d^4y j_\mu^a(x) D_{\mu\nu}(x-y) j_\nu^a(y) \quad (1)$$

where the quark currents,  $j_\mu^a(x) = \bar{q}(x) \frac{\lambda^a}{2} \gamma_\mu q(x)$ , interact via a phenomenological gluon two-point function ( $D_{\mu\nu}(x) = \delta_{\mu\nu} D(x)$  in the Feynman-like gauge chosen here). We consider only two flavors ( $u$  and  $d$ ) and use a Euclidean metric throughout, such that  $a \cdot b = a_\mu b_\mu$  and  $\{\gamma_\mu, \gamma_\nu\} = 2\delta_{\mu\nu}$ , with  $\gamma_\mu = \gamma_\mu^\dagger$ . The bare masses are represented by the diagonal matrix  $m = (m_u, m_d)$ . The closely related NJL model [12] is specified by the zero-range limit of Eq. (1) together with a set of coupling constants for the independent meson modes.

There has been extensive work on both the meson and baryon sectors that arise from hadronization of the GCM and a comprehensive review [25] is available. For just the lowest mass modes, the meson action for the effective local field variables  $\vec{\pi}, \vec{\rho}_\mu, \omega$  can be written as [10,11]

$$\begin{aligned} \hat{S}[\pi, \rho, \omega] = & \text{Tr} \sum_{n=2}^{\infty} \frac{(-)^n}{n} [S_0(i\gamma_5 \vec{\tau} \cdot \vec{\pi} \hat{\Gamma}_\pi + i\gamma_\mu \omega_\mu \hat{\Gamma}_V + i\gamma_\mu \vec{\tau} \cdot \vec{\rho}_\mu \hat{\Gamma}_V)]^n \\ & + 9 \int d^4x d^4y \frac{\frac{1}{2} \vec{\pi} \cdot \vec{\pi} \hat{\Gamma}_\pi^2 + \omega^2 \hat{\Gamma}_V^2 + \vec{\rho} \cdot \vec{\rho} \hat{\Gamma}_V^2}{2D(x-y)}. \end{aligned} \quad (2)$$

For completeness, we collect the main steps in the transition from Eq. (1) to Eq. (2) into the Appendix. In Eq. (2) Tr denotes the trace over color, flavor and spin as well as the continuous space-time variable. The quark propagator is  $S_0(p) = [i \not{p} A(p^2) + B(p^2) + m]^{-1}$ . The first term of Eq. (2) represents the sum of all possible meson couplings mediated by a single quark loop and the second term can be described as a contribution to the meson mass terms.

For simplicity, we have made the common approximation in Eq. (2) that each meson Bethe-Salpeter (BS) amplitude is truncated to its single canonical Dirac matrix covariant with  $\hat{\Gamma}$  being the associated scalar function. In studies of the BS equation that allow a more complete selection of covariants, [26,27] this is found to be the dominant component. In Eq. (2) we have also used the result that for the pure isospin components  $\hat{\Gamma}_\rho = \hat{\Gamma}_\omega$  which follows from the ladder BS equation when coupling terms generated from  $m_d - m_u$  are ignored. This defines the vector meson states of good isospin whose mixing we shall subsequently study. In a momentum representation the meson-quark coupling implicit in Eq. (2) is, e.g.,  $\bar{q}(q_+) i\gamma_\mu \omega_\mu(P) \hat{\Gamma}_V(q; P) q(q_-)$  where the quark momenta are  $q_\pm = q \pm P/2$  with  $P$  being the meson momentum. Thus  $\hat{\Gamma}_V(q; P)$  plays the role of a form factor but has, in principle, a well-defined dynamical content defined by the model at the quark-gluon level. In this work we utilize the dynamical structure of Eq. (2) to combine previous work on the pion sector with a phenomenological approach to  $\hat{\Gamma}_V$  to explore whether important features of the  $\rho - \omega$  system can be described.

### III. THE PION SECTOR

The free pion part of the action in Eq. (2) is

$$\hat{S}_2[\pi] = \frac{1}{2} \int \frac{d^4 P}{(2\pi)^4} \vec{\pi}(-P) \cdot \vec{\pi}(P) \hat{\Delta}_\pi^{-1}(P^2), \quad (3)$$

where the inverse propagator for the effective local pion field is

$$\hat{\Delta}_\pi^{-1}(P^2) = \text{tr} \int \frac{d^4 q}{(2\pi)^4} [S_0(q_-) i\gamma_5 \tau S_0(q_+) i\gamma_5 \tau] \hat{\Gamma}_\pi^2(q; P) + \frac{9}{2} \int d^4 r \frac{\hat{\Gamma}_\pi^2(r; P)}{D(r)}. \quad (4)$$

Here  $q_\pm = q \pm \frac{P}{2}$  and  $\tau$  is any single component of  $\vec{\tau}$ . Throughout this work the symbol  $\text{tr}$  denotes a trace over color, flavor ( $N_f = 2$ ) and spin. We note that  $\hat{\Delta}_\pi^{-1}$  is a functional of  $\hat{\Gamma}_\pi$  and that  $\delta \hat{\Delta}_\pi^{-1} / \delta \hat{\Gamma}_\pi = 0$  is the ladder BS equation (projected onto the  $i\gamma_5 \tau$  channel) for the amplitude  $\hat{\Gamma}_\pi$ . To produce  $\hat{\Gamma}_\pi$  that way requires a specification of the model gluon propagator. However an indirect route is provided through chiral symmetry by the Goldstone theorem in terms of the dressed quark propagator. The realization relevant to the present treatment is that, in the chiral limit, the ladder BS equation for the amplitude  $\hat{\Gamma}_\pi(q; P)$  becomes identical to the ladder Dyson-Schwinger equation for  $B_0(q^2) \equiv B(q^2; m = 0)$ , the scalar part of the dynamically generated quark self-energy [28]. Thus the chiral limit pion, in this approach, is automatically both a massless Goldstone boson and a finite size  $q\bar{q}$  bound state. For a small bare mass, numerical studies [29] reveal that  $\hat{\Gamma}_\pi$  is still well approximated by the scalar quark self-energy amplitude.

In this work we take  $\hat{\Gamma}_\pi(q; P) \approx B(q^2; m)$  and use  $m_{av} = (m_u + m_d)/2$  as the bare mass for both the  $u$  and  $d$ . Near the mass shell, we have the general form  $\hat{\Delta}_\pi^{-1}(P^2) = (P^2 + m_\pi^2) f_\pi^2$ , where  $f_\pi$  is the pion wavefunction renormalization constant. The (constant) second term of Eq. (4) may therefore be eliminated if we require that the GMOR relation [30] in the form  $\Delta_\pi^{-1}(0) = 2m_{av} |\langle \bar{q}q \rangle|$  be satisfied. Here  $\langle \bar{q}q \rangle$  is the isospin average vacuum condensate. In this regard we note that recent investigations [29,31] find that a somewhat differently defined quantity is better suited to this relation. The numerical consequences for the present work are not significant. Our procedure yields

$$\hat{\Delta}_\pi^{-1}(P^2) = 2m_{av} |\langle \bar{q}q \rangle| - \text{tr} \int \frac{d^4 q}{(2\pi)^4} [S_0(q_-) S_0(-q_+) - S_0(q) S_0(-q)] B^2(q^2), \quad (5)$$

where we take  $|\langle \bar{q}q \rangle| = \frac{1}{2} \text{tr} \int^{\mu^2} \frac{d^4 q}{(2\pi)^4} S_0(q)$  with the scale specified by the cutoff  $\mu^2 = 1 \text{ GeV}^2$ . Now  $\hat{\Delta}_\pi^{-1}$  is fully specified in terms of the quark propagator. Numerical evaluation of Eq. (5) identifies the pion mass through the zero at  $P^2 = -m_\pi^2$ .

We also identify  $Z_\pi(P^2)$  defined by  $\hat{\Delta}_\pi^{-1}(P^2) = (P^2 + m_\pi^2) Z_\pi(P^2)$ . The momentum dependence of  $Z_\pi(P^2)$  implies a dynamical mass function  $m_\pi(P^2)$  due to  $\bar{q}q$  substructure. We calculate  $f_\pi$  from  $f_\pi^2 = Z_\pi(P^2 = -m_\pi^2)$ . A physical normalization (unit residue at the mass-shell pole) is produced by absorbing  $f_\pi$  into the pion fields. For convenience, we redefine the fields to absorb  $\sqrt{Z_\pi(P^2)}$  so that the propagator becomes  $\Delta_\pi = (P^2 + m_\pi^2)^{-1}$ . The associated vertex amplitude is then the dimensionless quantity  $\Gamma_\pi(p; P) = B(p^2) / \sqrt{Z_\pi(P^2)}$ .

At the mass-shell this procedure satisfies the canonical Bethe-Salpeter normalization condition [32]. For any pion momentum, this choice defines the effective pion-quark vertex and related pion field consistent with the point-pion propagator  $\Delta_\pi = (P^2 + m_\pi^2)^{-1}$  to allow contact with common procedures in nuclear physics. In various applications we test the role of the composite nature of the pion in by replacing the function  $Z_\pi(P^2)$  by its mass-shell value  $Z_\pi(-m_\pi^2)$ . Such tests will be described later.

For the dressed quark propagator, we use the representation  $S_0(p) = -i\gamma \cdot p \sigma_V(p^2) + \sigma_S(p^2)$ , and employ the following simplified form of previously developed parameterized amplitudes [1]

$$\bar{\sigma}_S(x) = c(\bar{m}) e^{-2x} + \frac{\bar{m}}{x} (1 - e^{-2x}), \quad (6)$$

$$\bar{\sigma}_V(x) = \frac{2x - 1 + e^{-2x}}{2x^2} - c(\bar{m}) \bar{m} e^{-2x}, \quad (7)$$

with  $x = p^2/\lambda^2$ ,  $\bar{\sigma}_S = \lambda\sigma_S$ ,  $\bar{\sigma}_V = \lambda^2\sigma_V$ ,  $\bar{m} = m/\lambda$ , where  $m$  is the bare quark mass and  $\lambda$  is the momentum scale. This  $S_0(p)$  is an entire function in the complex momentum plane, a condition sufficient to ensure the absence of quark production thresholds in S-matrix amplitudes for physical processes [33]. The original parameterization is guided by a confining model DSE [34] and by the behavior found in realistic DSE studies [3,35]. It is consistent with pQCD in the deep Euclidean region apart from  $\ln(p^2)$  corrections. The parameters are  $\lambda = 0.889$  GeV,  $c(\bar{m}_{av}) = c_0 = 0.581$ ,  $m_{av} = 16$  MeV. The soft chiral physics quantities produced by these parameters are  $f_\pi = 90.1$  MeV,  $m_\pi = 143$  MeV, and  $\langle \bar{q}q \rangle = (173 \text{ MeV})^3$ . The more elaborate original parameterization [1] provides a better fit to the above and also an excellent description of the pion electromagnetic form factor and the  $\pi\pi$  scattering lengths.

With the isoscalar quark propagator set as above, the isovector term is generated from the bare mass dependence by substitution of  $\bar{m} = \bar{m}_{av} + \frac{\tau_3}{2}\delta\bar{m}$  with  $\delta\bar{m} = \bar{m}_u - \bar{m}_d$ . The constant  $c(\bar{m})$  mainly represents the strength of dynamical chiral symmetry breaking that generates the dynamical mass function,  $M(p^2) = \sigma_S(p^2)/\sigma_V(p^2)$ . However a weak bare mass dependence for  $c(\bar{m})$  is necessary to simulate the bare mass dependence of realistic DSE solutions. This leads to a small isovector component of  $c(\bar{m})$  and we write  $c(\bar{m}) = c_0 + \tau_3 c_1$ , where  $c_0 = c(\bar{m}_{av})$  is given above, and  $c_1 = (c_u - c_d)/2$ . To determine the latter we fit to the bare mass dependence of  $\bar{\sigma}_S(p^2 = 0)$  produced by realistic DSE studies [35]. Only a linear behavior  $c_1 = d\delta\bar{m}/2$  characterized by the slope  $d = c'(\bar{m}) < 0$  is important, and with  $\delta m = -4$  MeV, we have  $c_1 = 0.0048$ . This 1% isospin-breaking effect  $c_1/c_0$  is of the order of magnitude expected. The quark propagator can be written as  $S_0(p) = S_0^0(p) + \tau_3 S_0^1(p)$  where the latter isovector component is responsible for the various  $\rho^0 - \omega$  mixing mechanisms considered here.

#### IV. THE $\rho - \omega$ SECTOR AT TREE LEVEL

We treat the transverse modes in the  $\rho$  and  $\omega$  channels and use fields that contain the transverse projector  $T_{\mu\nu}(P) = \delta_{\mu\nu} - P_\mu P_\nu / P^2$ . That is,  $\vec{\rho}_\mu(P) \equiv T_{\mu\nu}(P)\vec{\rho}_\nu(P)$  and  $\omega_\mu(P) \equiv T_{\mu\nu}(P)\omega_\nu(P)$ . In a matrix notation where  $V_\mu$  denotes  $(\vec{\rho}_\mu, \omega_\mu)$ , the tree-level action from Eq. (2), up to second order in the fields, can be written as

$$\hat{S}_2[\rho, \omega] = \frac{1}{2} \int \frac{d^4 P}{(2\pi)^4} V_\mu^T(-P) [\hat{\Delta}_{\mu\nu}^{-1}(P) + \hat{\Pi}_{\mu\nu}^q(P)] V_\nu(P). \quad (8)$$

Here, in meson channel space,  $\hat{\Delta}^{-1}$  is diagonal and the only non-zero elements of  $\hat{\Pi}^q$  are the off-diagonal ones that provide  $\rho^0 - \omega$  coupling. The superscript  $q$  identifies the quark-loop contribution to distinguish from a different contribution introduced later. The diagonal inverse propagator is given by

$$\hat{\Delta}_{\mu\nu}^{-1}(P) = \text{tr} \int \frac{d^4 q}{(2\pi)^4} \hat{\Gamma}_V^2(q; P) [S_0(q_-) i\gamma_\mu f S_0(q_+) i\gamma_\nu f] + 9 \delta_{\mu\nu} \int d^4 r \frac{\hat{\Gamma}_V^2(r; P)}{D(r)}. \quad (9)$$

Here  $f$  are the relevant flavor factors ( $1_f$  for the  $\omega$ , and  $\vec{\tau}$  for the  $\vec{\rho}$ ) and  $q_\pm = q \pm \frac{P}{2}$ , where  $P$  is the meson momentum and  $q$  is the loop momentum, or equivalently the  $\bar{q}q$  relative momentum. The amplitude  $\hat{\Gamma}_V$  is defined in the diagonal sector by the ladder BS equation produced by  $\delta\hat{\Delta}^{-1}/\delta\hat{\Gamma}_V = 0$ . Thus  $\hat{\Gamma}_V$  contains no isospin mixing mechanism and is the same for  $\rho$  and  $\omega$ . The diagonal  $\rho$  and  $\omega$  elements of the inverse propagator are likewise identical. The transverse component  $\hat{\Delta}^{-1}(P^2)$ , defined by  $\hat{\Delta}_{\mu\nu}^{-1}(P) = T_{\mu\nu}(P) \hat{\Delta}^{-1}(P^2)$ , is given explicitly by

$$\begin{aligned} \hat{\Delta}^{-1}(P^2) = & 24 \int \frac{d^4 q}{(2\pi)^4} \hat{\Gamma}_V^2(q; P) \left\{ \sigma_V(q_+^2) \sigma_V(q_-^2) \left[ \frac{P^2}{4} + \frac{q^2}{3} - \frac{2(P \cdot q)^2}{3P^2} \right] - \sigma_S(q_+^2) \sigma_S(q_-^2) \right\} \\ & + 9 \int d^4 r \frac{\hat{\Gamma}_V^2(r; P)}{D(r)}. \end{aligned} \quad (10)$$

Here we have ignored a small contribution from the isovector component of the quark propagator by using  $m_{av}$  as the bare quark mass.

The mixed self-energy,  $\hat{\Pi}_{\mu\nu}^q(P)$ , is produced from the same quark loop term of the effective action of Eq. (2) that produces  $\hat{\Delta}_{\mu\nu}^{-1}$ . The mechanism is illustrated in Fig. 1. The explicit expression is

$$\hat{\Pi}_{\mu\nu}^q(P) = \text{tr} \int \frac{d^4 q}{(2\pi)^4} [S_0(q_-) i\gamma_\mu \tau_3 S_0(q_+) i\gamma_\nu] \hat{\Gamma}_V^2(q; P), \quad (11)$$

which is identical to the first term of Eq. (9) except that one of the flavor factors is  $\tau_3$  and the other is  $1_f$ . Thus,  $\hat{\Pi}_{\mu\nu}^q(P)$  is nonzero only if  $S_0$  has an isovector component. The structure of Eq. (11) corresponds to first-order perturbation theory for isospin breaking effects in that the internal meson states or BS amplitudes that enter are from the unperturbed or isospin symmetric sector. The mixed self-energy may be expressed as the difference of quark loops and the leading contribution is proportional to  $\delta m$ . The transverse component is  $\hat{\Pi}^q(P^2) = \hat{\Pi}_u - \hat{\Pi}_d$ , where

$$\hat{\Pi}_f(P^2) = 12 \int \frac{d^4 q}{(2\pi)^4} \hat{\Gamma}_V^2(q; P) \left\{ \sigma_V^f(q_+^2) \sigma_V^f(q_-^2) \left[ \frac{P^2}{4} + \frac{q^2}{3} - \frac{2(P \cdot q)^2}{3P^2} \right] - \sigma_S^f(q_+^2) \sigma_S^f(q_-^2) \right\}. \quad (12)$$

To summarize the transverse  $\rho^0 - \omega$  sector, the inverse propagator obtained at the quark loop level may be written as

$$\hat{\mathcal{D}}^{-1}(P^2) = \begin{pmatrix} \hat{\Delta}^{-1}(P^2) & \hat{\Pi}^q(P^2) \\ \hat{\Pi}^q(P^2) & \hat{\Delta}^{-1}(P^2) \end{pmatrix}. \quad (13)$$

We shall refer to the basis here as  $(\rho_I^0, \omega_I)$  to indicate pure isospin states.

The composite  $\bar{q}q$  nature of the mesons is reflected in the fact that the diagonal elements contain a dynamical mass function. The general form

$$\hat{\Delta}^{-1}(P^2) = (P^2 + m_V^2)Z_1(P^2) = (P^2 + m_V^2(P^2)) \quad (14)$$

identifies the degenerate mass  $m_V$  of the  $\rho_I^0$  and  $\omega_I$  states. It is convenient to carry out part of the necessary renormalization at this stage. Without the off-diagonal terms of Eq. (13), a physical normalization (unit residue at the mass-shell pole) would be produced by absorbing at least the on-mass-shell value of  $\sqrt{Z_1}$  into the fields. As with the pion sector, we choose to absorb the function  $\sqrt{Z_1(P^2)}$  into the fields so that the resulting unmixed propagators have the standard point meson form. The associated BS amplitudes are now  $\Gamma_V(q; P) = \hat{\Gamma}_V(q; P)/\sqrt{Z_1(P^2)}$ , which are dimensionless quantities that, at the mass-shell, satisfy the standard normalization condition [32] for a BS amplitude. We note that the meson- $\bar{q}q$  coupling strength (magnitude of  $\Gamma_V$  at the meson mass-shell) is thus a prediction of this approach. The quark loop contribution to the  $\rho^0 - \omega$  sector is now

$$\mathcal{D}^{-1}(P^2) = \begin{pmatrix} P^2 + m_V^2 & \Pi^q(P^2) \\ \Pi^q(P^2) & P^2 + m_V^2 \end{pmatrix}, \quad (15)$$

where  $\Pi^q(P^2) = \hat{\Pi}^q(P^2)/Z_1(P^2)$ . The role played by the dynamical  $\bar{q}q$  substructure of propagators may be obtained by holding the function  $Z_1(P^2)$  at its on-mass-shell value to simulate a structureless meson.

To facilitate these exploratory calculations, we adopt the simple form  $\hat{\Gamma}_V(q; P) = N \exp(-q^2/a^2)$  which has previously been found to provide an adequate one-parameter representation of the relevant BS amplitude in a variational approach [25]. The physical amplitude  $\Gamma_V$  is independent of  $N$ . The choice of effective gluon propagator  $D(r)$  in Eq. (10) is made indirectly by ensuring that the resulting constant value of the second term produces a zero in  $\hat{\Delta}^{-1}(P^2)$  at  $P^2 = -m_V^2$  where  $m_V = m_\omega = 782$  MeV. The range parameter  $a$  is chosen to reproduce the empirical value of  $g_{\rho\pi\pi}$  as discussed in the next Section.

The transverse mixing amplitude  $\Pi^q(P^2)$  obtained from this approach has been discussed in a previous work [9]. The present parameterization of the input to this model is slightly different but only small quantitative changes occur in the calculated  $\Pi^q(P^2)$  and the conclusions of our previous work remain unchanged.

## V. THE $\rho\pi\pi$ AND $\omega\pi\pi$ INTERACTIONS

From the effective action in Eq. (2), we identify the interaction term

$$S[\rho\pi\pi] = -\text{Tr} \left[ S_0 i\gamma_\mu \vec{\tau} \cdot \vec{\rho}_\mu \Gamma_V (S_0 i\gamma_5 \vec{\tau} \cdot \vec{\pi} \Gamma_\pi)^2 \right]. \quad (16)$$

Use of the momenta shown in the quark triangle diagram of Fig. 2 yields the explicit expression



$$S[\rho\pi\pi] = i \int \frac{d^4 P, Q}{[(2\pi)^4]^2} \vec{\rho}_\mu(Q) \cdot \vec{\pi}(-P - \frac{Q}{2}) \times \vec{\pi}(P - \frac{Q}{2}) \Lambda_\mu^\rho(P, Q), \quad (17)$$

where the vertex is

$$\Lambda_\mu^\rho(P, Q) = \int \frac{d^4 k}{(2\pi)^4} \Gamma_V(k + \frac{P}{2}; Q) \Gamma_\pi(k + \frac{Q}{4}; -P - \frac{Q}{2}) \Gamma_\pi(k - \frac{Q}{4}; P - \frac{Q}{2}) T_\mu(k, P, Q) \quad (18)$$

with the discrete loop trace denoted by

$$T_\mu(k, P, Q) = \text{tr} \left[ S_0(k + \frac{P}{2} + \frac{Q}{2}) i\gamma_\mu S_0(k + \frac{P}{2} - \frac{Q}{2}) i\gamma_5 S_0(k - \frac{P}{2}) i\gamma_5 \right]. \quad (19)$$

The symmetry properties of  $\Lambda_\mu^\rho(P, Q)$  that follow are  $\Lambda_\mu^\rho(P, Q) = -\Lambda_\mu^\rho(-P, Q) = \Lambda_\mu^\rho(P, -Q)$ . Hence the most general form is

$$\Lambda_\mu^\rho(P, Q) = -P_\mu F_{\rho\pi\pi}(P^2, Q^2, (P \cdot Q)^2) - Q_\mu P \cdot Q H_{\rho\pi\pi}(P^2, Q^2, (P \cdot Q)^2). \quad (20)$$

With both pions on the mass-shell,  $(P - \frac{Q}{2})^2 = (P + \frac{Q}{2})^2 = -m_\pi^2$ . Equivalently,  $P \cdot Q = 0$  and  $P^2 = -m_\pi^2 - \frac{Q^2}{4}$  so that the simplified form of Eq. (20) is  $\Lambda_\mu^\rho(P, Q) = -P_\mu F_{\rho\pi\pi}(Q^2)$ . The coupling constant is defined as the mass-shell value  $g_{\rho\pi\pi} = F_{\rho\pi\pi}(Q^2 = -m_\rho^2)$ . If the form factor is held at this value for all momenta, one obtains the point coupling limit

$$S[\rho\pi\pi] = -ig_{\rho\pi\pi} \int \frac{d^4 P, Q}{[(2\pi)^4]^2} P_\mu \vec{\rho}_\mu(Q) \cdot \vec{\pi}(-P - \frac{Q}{2}) \times \vec{\pi}(P - \frac{Q}{2}). \quad (21)$$

which is equivalent to the more standard form

$$S[\rho\pi\pi] = -g_{\rho\pi\pi} \int d^4 x \vec{\rho}_\mu(x) \cdot \vec{\pi}(x) \times \partial_\mu \vec{\pi}(x). \quad (22)$$

With the parameterized BS amplitude  $\Gamma_V(q; P) \propto \exp(-q^2/a^2)$ , we take  $a = 0.194 \text{ GeV}^2$  to reproduce the value  $g_{\rho\pi\pi}^{\text{expt}} = 6.05$  as inferred from the experimental  $\rho \rightarrow \pi\pi$  decay width of 151 MeV. The calculated form factor  $F_{\rho\pi\pi}(Q^2)$  is displayed in Fig. 3 for timelike and spacelike momenta in the vicinity of the mass-shell. A previous study [20] within the GCM made the approximation  $g_{\rho\pi\pi} \approx F_{\rho\pi\pi}(P = Q = 0)$  to avoid the occurrence of complex momenta in the arguments of propagators and vertex functions in the quark loop. From Fig. 3 it is evident this approximation can underestimate the value by almost a factor of two.

The pion loop mechanism to be considered later requires the  $\rho\pi\pi$  vertex for off-shell pion momenta. Only the form factor  $F_{\rho\pi\pi}$  is relevant due to the transverse  $\rho$  condition. Results from numerical evaluation of Eq. (18) over the relevant range of  $P^2$  and  $Q^2$  for  $P \cdot Q = 0$  are displayed in Fig. 4. For later use we parameterize the results in the form

$$F_{\rho\pi\pi}(P^2, Q^2) \approx f_{\rho\pi\pi}(Q^2) e^{-P^2/\lambda_\rho^2(Q^2)}. \quad (23)$$

The constraint  $P \cdot Q = 0$  is applied to facilitate subsequent use in the  $\pi$  loop integral and it is exact at the important on-mass-shell point for both pions. The functions  $f_{\rho\pi\pi}(Q^2)$  and  $\lambda_\rho(Q^2)$  are chosen to provide a fit to the calculated  $\rho$  momentum dependence of the

vertex to within 1% for  $Q^2$  between  $-m_\rho^2$  and 0.6 GeV<sup>2</sup>. We use  $f_{\rho\pi\pi}(Q^2) = \sum_{n=0}^2 a_n z^n$  and  $\lambda_\rho(Q^2) = \mu \sum_{n=0}^6 b_n z^n$  with  $z = Q^2/\mu^2$  and  $\mu = 1$  GeV. The parameters are  $(a_0, a_1, a_2) = (3.04, -5.20, 2.37)$  and  $(b_0, \dots, b_6) = (1.28, 0.252, 0.110, 0.171, 1.08, 1.80, 0.865)$ .

The  $\omega\pi\pi$  interaction term from the effective action of Eq. (2) is

$$S[\omega\pi\pi] = -Tr \left[ S_0 i\gamma_\mu \omega_\mu \Gamma_V (S_0 i\gamma_5 \vec{\tau} \cdot \vec{\pi} \Gamma_\pi)^2 \right]. \quad (24)$$

This is identical in form to the  $\rho\pi\pi$  interaction except for the isospin structure. If the only isovector quantities involved here are the pion fields, the resulting expression is just Eq. (17) but with isospin structure  $\vec{\pi} \cdot \vec{\pi}$ . The symmetry properties of  $\Lambda_\mu^\omega(P, Q)$  then show that the result is identically zero as required by G-parity conservation. With extra isovector components provided by the quark propagators, the G-parity violating result is

$$\hat{S}_3[\omega\pi\pi] = i \int \frac{d^4 P, Q}{[(2\pi)^4]^2} \omega_\nu(Q) \hat{3} \cdot \vec{\pi}(-P - Q/2) \times \vec{\pi}(P - Q/2) \Lambda_\nu^\omega(P; Q), \quad (25)$$

where the vertex is

$$\Lambda_\mu^\omega(P, Q) = \int \frac{d^4 k}{(2\pi)^4} \Gamma_V(k + \frac{P}{2}; Q) \Gamma_\pi(k + \frac{Q}{4}; -P - \frac{Q}{2}) \Gamma_\pi(k - \frac{Q}{4}; P - \frac{Q}{2}) N_\mu(k, P, Q). \quad (26)$$

Here, to lowest order in isospin breaking, the loop trace is proportional to  $\delta m$  and is given by  $N_\mu = N_\mu^{100} - N_\mu^{001} + N_\mu^{010}$ , where

$$N_\mu^{abc}(k, P, Q) = \text{tr} \left[ S_0^a(k + \frac{P}{2} + \frac{Q}{2}) i\gamma_\mu S_0^b(k + \frac{P}{2} - \frac{Q}{2}) i\gamma_5 S_0^c(k - \frac{P}{2}) i\gamma_5 \right], \quad (27)$$

with the isospin components of the propagators defined by  $S_0 = S_0^0 + \tau_3 S_0^1$ .

The symmetry properties of  $\Lambda_\mu^\omega(P, Q)$  are identical to those for  $\Lambda_\mu^\rho(P, Q)$  and hence the general form is

$$\Lambda_\mu^\omega(P, Q) = -P_\mu F_{\omega\pi\pi}(P^2, Q^2, (P \cdot Q)^2) - Q_\mu P \cdot Q H_{\omega\pi\pi}(P^2, Q^2, (P \cdot Q)^2). \quad (28)$$

At the triple on-mass-shell point, numerical evaluation of  $F_{\omega\pi\pi}$  yields the coupling constant  $g_{\omega_I\pi\pi} = 0.105$ . This is almost five times larger than the value 0.0236 recently obtained in Ref. [15]. The  $2\pi$  width of the physical  $\omega$  is 0.185 MeV which implies  $g_{\omega\pi\pi}^{expt} = 0.21$ . The theoretical quantity  $g_{\omega_I\pi\pi}$  obtained so far refers to the pure isospin  $\omega_I$  state and a small admixture of  $\rho_I$  can make a significant contribution to the physical  $\omega \rightarrow 2\pi$  decay. We will return to this topic later. The calculated off-shell form factor  $F_{\omega\pi\pi}(P^2, Q^2)$  is displayed in Fig. 5 for  $P \cdot Q = 0$ . A common assumption is that the  $\rho\pi\pi$  and  $\omega\pi\pi$  form factors simply scale by the ratio of their coupling constants so that the pion loop  $\rho^0 - \omega$  self-energy may be estimated by scaling the corresponding  $\rho$  self-energy [21,36]. From Figs. 4 and 5 the present calculations show that this can be qualitatively reliable for momenta where the form factors are significant. The departures that do occur are due to the different momentum dependence of the isoscalar and isovector components of the quark propagator.

For the subsequent pion loop calculation we parameterize the  $\omega\pi\pi$  form factor in the same way as in Eq. (23). That is,  $f_{\omega\pi\pi}(Q^2) = \sum_{n=0}^2 a_n z^n$  and  $\lambda_\omega(Q^2) = \mu \sum_{n=0}^6 b_n z^n$  with  $z = Q^2/\mu^2$  and  $\mu = 1$  GeV. The parameters are  $(a_0, a_1, a_2) = (7.07, -6.91, 3.21) \times 10^{-2}$  and  $(b_0, \dots, b_6) = (118, 6.76, -1.72, -0.391, -0.172, 0.109, 0.140) \times 10^{-2}$ .

## VI. THE $\rho - \omega$ SECTOR UP TO ONE-PION-LOOP

The relevant low-order terms in the effective action for  $\pi, \rho, \omega$  that we have produced by integrating out the quarks are

$$\hat{S}[\pi, \rho, \omega] = \hat{S}_2[\rho, \omega] + \hat{S}_2[\pi] + \hat{S}[\rho\pi\pi] + \hat{S}[\omega\pi\pi] + \dots \quad (29)$$

Here the second-order terms  $\hat{S}_2[\rho, \omega]$  and  $\hat{S}_2[\pi]$  represent respectively the  $\rho - \omega$  sector containing the quark-loop mixing mechanism and the free pion sector. To integrate out the pion fields, it is convenient to first combine the last three terms of Eq. (29) so that it becomes

$$\hat{S}[\pi, \rho, \omega] = \hat{S}[\rho, \omega] + \frac{1}{2} \int \frac{d^4 P, P'}{(2\pi)^8} \pi_i(P') D_{ij}^{-1}(P', P) \pi_j(P). \quad (30)$$

The three terms in

$$D_{ij}^{-1}(P', P) = \Delta_{ij}^{-1}(P', P) + V_{ij}(P', P) + W_{ij}(P', P) \quad (31)$$

correspond to the free pion term given by

$$\Delta_{ij}^{-1}(P', P) = (2\pi)^4 \delta_{ij} \delta^4(P' + P) \Delta_\pi^{-1}(P^2), \quad (32)$$

the  $\rho\pi\pi$  interaction term given by

$$V_{ij}(P', P) = 2i\epsilon_{ijk} \rho_\mu^k(-P' - P) \Lambda_\mu^\rho(-\frac{P' + P}{2}; -P' - P), \quad (33)$$

and the  $\omega\pi\pi$  interaction term given by

$$W_{ij}(P', P) = 2i\epsilon_{ij3} \omega_\mu(-P' - P) \Lambda_\mu^\omega(-\frac{P' + P}{2}; -P' - P). \quad (34)$$

Integration over the pion fields allows a new effective action  $\hat{\mathcal{S}}[\rho, \omega]$  to be identified from

$$Z = N \int D\rho D\omega D\pi \exp(-\hat{S}[\pi, \rho, \omega]) = N' \int D\rho D\omega \exp(-\hat{\mathcal{S}}[\rho, \omega]) \quad (35)$$

by using the functional integral result

$$\int D\pi \exp\left(-\frac{1}{2} \int \frac{d^4 P, P'}{(2\pi)^8} \pi_i(P') D_{ij}^{-1}(P', P) \pi_j(P)\right) = \exp\left(-\frac{1}{2} \text{TrLn } D^{-1}\right). \quad (36)$$

We absorb the field-independent term  $\exp(-\frac{1}{2} \text{TrLn } \Delta^{-1})$  into the normalization constant to arrive at

$$\hat{\mathcal{S}}[\rho, \omega] = \hat{S}_2[\rho, \omega] + \frac{1}{2} \text{TrLn}(1 + \Delta(V + W)). \quad (37)$$

The second term here gives the vector meson coupling to all orders produced by a single pion loop.

The quadratic part of the second term of Eq. (37) adds a contribution to the vector meson inverse propagator to that given previously by Eq. (15) at the quark loop level. In the transverse  $\rho^0 - \omega$  sector, the net result for the inverse propagator is

$$\mathcal{D}^{-1}(P^2) = \begin{pmatrix} P^2 + m_V^2 + \Pi^{\rho\rho}(P^2) & \Pi^{\rho\omega}(P^2) \\ \Pi^{\rho\omega}(P^2) & P^2 + m_V^2 + \Pi^{\omega\omega}(P^2) \end{pmatrix}, \quad (38)$$

where the net mixing amplitude is  $\Pi^{\rho\omega}(P^2) = \Pi^q(P^2) + \Pi^\pi(P^2)$ . The additional terms produced by the pion loop are the diagonal elements  $\Pi^{\rho\rho}(P^2)$  and  $\Pi^{\omega\omega}(P^2)$ , and the mixing term  $\Pi^\pi(P^2)$ . From Eq. (37), the self-energy contribution  $\Pi^{\rho\rho}(P^2)$  is given by the transverse component of

$$\Pi_{\mu\nu}^{\rho\rho}(P) = -4 \int \frac{d^4 q}{(2\pi)^4} \Delta_\pi(q_+) \Delta_\pi(q_-) \Lambda_\mu^\rho(q; -P) \Lambda_\nu^\rho(q; P), \quad (39)$$

where  $q_\pm = q \pm P/2$ , and the summation over pion isospin labels has been carried out. This contribution is the same for each isospin component of the  $\rho$ . Similarly, the mixed  $\rho^0 - \omega$  self-energy contribution generated by the pion loop is given by

$$\Pi_{\mu\nu}^\pi(P) = -4 \int \frac{d^4 q}{(2\pi)^4} \Delta_\pi(q_+) \Delta_\pi(q_-) \Lambda_\mu^\rho(q; -P) \Lambda_\nu^\omega(q; P), \quad (40)$$

and  $\Pi^\pi(P^2)$  is the transverse component of that. The  $\omega$  self-energy contribution is obtained from Eq. (39) by the replacement of  $\Lambda^\rho$  by  $\Lambda^\omega$ . It is quadratic in the small symmetry breaking mechanism and is ignored here.

In the absence of mixing, the real part of  $\Pi^{\rho\rho}(P^2)$  generates a mass shift for the isospin eigenstate  $\rho_I$ . Since the corresponding quantity in the  $\omega_I$  channel is much smaller, and neglected in this work, this mass shift represents the  $\rho - \omega$  mass splitting. For timelike momenta such that  $P^2 \leq -4m_\pi^2$ , both  $\Pi^{\rho\rho}(P^2)$  and  $\Pi^\pi(P^2)$  have imaginary parts associated with the decay  $\rho \rightarrow 2\pi$ . The imaginary part of  $\Pi^{\rho\rho}(P^2)$  produces the  $2\pi$  width of the  $\rho_I$  state.

These observations are, in principle, modified by the presence of nonzero off-diagonal elements in Eq. (38). To see this, we construct the eigenvalues of the inverse meson propagator,  $\mathcal{D}^{-1}(P^2)$ . These are, to lowest order in the total mixing amplitude, given by the expressions  $\lambda_\rho(P^2) = P^2 + m_V^2 + \Pi^{\rho\rho}(P^2)(1 + \epsilon^2(P^2))$ , and  $\lambda_\omega(P^2) = P^2 + m_V^2 - \Pi^{\rho\rho}(P^2)\epsilon^2(P^2)$ , where

$$\epsilon(P^2) = -\frac{\Pi^{\rho\omega}(P^2)}{\Pi^{\rho\rho}(P^2)} \quad (41)$$

is a natural measure of off-diagonal coupling. Since the typical size is  $|\epsilon| \approx 0.03$  in the mass-shell region, we shall ignore the second order mixing effects on the mass shifts. In the diagonal basis we therefore have, through first order in mixing,

$$\mathcal{D}^{-1}(P^2) = \begin{pmatrix} P^2 + m_\omega^2 + \Pi^{\rho\rho}(P^2) & 0 \\ 0 & P^2 + m_\omega^2 \end{pmatrix}, \quad (42)$$

where we have made the identification  $m_\omega = m_V$ . We identify the mass of the (mixed)  $\rho$  eigenstate from the position of the zero in the real part of the upper eigenvalue in Eq. (42). That is,

$$m_\rho^2 = m_\omega^2 + \text{Re } \Pi^{\rho\rho}(-m_\rho^2). \quad (43)$$

With the definition  $\hat{\Gamma}(P^2) = -\text{Im } \Pi^{\rho\rho}(P^2)/m_\rho$ , the inverse propagator in the  $\rho$  channel can be written as

$$\mathcal{D}_\rho^{-1}(P^2) = (P^2 + m_\rho^2 - im_\rho\Gamma(P^2)) Z_2(P^2), \quad (44)$$

where  $\Gamma(P^2) = \hat{\Gamma}(P^2)/Z_2(P^2)$ . The function  $Z_2(P^2)$  arises from the momentum dependence of the real part of the pion loop self-energy. The on-mass-shell value, which is to be absorbed into the  $\rho$  field as a renormalization constant, is given by

$$Z_2(-m_\rho^2) = 1 + \text{Re } \Pi^{\rho\rho'}(-m_\rho^2), \quad (45)$$

with the prime superscript denoting differentiation with respect to the argument. We choose to absorb the function  $\sqrt{Z_2(P^2)}$  into the field  $\rho_\mu(P)$  so that the resulting propagator has the conventional Breit-Wigner form. The physical width is given by

$$\Gamma_\rho = -\frac{\text{Im } \Pi^{\rho\rho}(-m_\rho^2)}{m_\rho Z_2(-m_\rho^2)}. \quad (46)$$

Our numerical results for the  $\rho$  mass shift and width are obtained from Eq. (39) in the specific form

$$\Pi^{\rho\rho}(P^2) = -\frac{4}{3}f_{\rho\pi\pi}^2(P^2) \int \frac{d^4q}{(2\pi)^4} \frac{(q^2 - (q \cdot P)^2/P^2)e^{-2q^2/\lambda_\rho^2(P^2)}}{\left[(q + \frac{P}{2})^2 + m_\pi^2 - i\epsilon\right] \left[(q - \frac{P}{2})^2 + m_\pi^2 - i\epsilon\right]}, \quad (47)$$

where the parameterized  $\rho\pi\pi$  vertex functions from Eq. (23) have been used. After reduction to a two-dimensional integral it is convenient to employ the Feynman combination of denominators to obtain

$$\Pi^{\rho\rho}(P^2) = -\frac{4}{3}f_{\rho\pi\pi}^2(P^2) \int_{-\frac{1}{2}}^{+\frac{1}{2}} d\alpha \int_0^\infty ds s^2 \int_{-1}^{+1} dz \sqrt{1-z^2} \frac{e^{-2(s-2\alpha z s P + \alpha^2 P^2)/\lambda_\rho^2(P^2)}}{\left[s + m_\pi^2 + \frac{P^2}{4} - \alpha^2 P^2 - i\epsilon\right]^2}. \quad (48)$$

The numerical results for  $\text{Re } \Pi^{\rho\rho}(P^2)$  and  $\text{Im } \Pi^{\rho\rho}(P^2)$  are shown in Fig. 6. The self-consistent solution for  $m_\rho$  produced by Eq. (43) is displayed in Fig. 7 in the following way. The quantity  $-(P^2 + m_\omega^2)$  is plotted as a long dash line and its intercept with the solid line representing  $\text{Re } \Pi^{\rho\rho}(P^2)$  identifies the mass shell point. We use  $m_\omega = m_V = 782$  MeV and find  $m_\rho = 761$  MeV giving  $m_\rho - m_\omega = -21$  MeV. The experimental value is  $-12.0 \pm 0.8$  MeV. At this mass-shell point we find  $\Pi^{\rho\rho}(-m_\rho^2) = -0.031 - 0.11i$  GeV<sup>2</sup>. The calculated field renormalization constant from Eq. (45) is  $Z_2(-m_\rho^2) = 0.90$ . Then Eq. (46) yields the width  $\Gamma_\rho = 156$  MeV while the experimental value is 151 MeV.

Fig. 7 also illustrates the contribution to the mass splitting result made by the momentum dependence of the meson self-energies generated by the  $\bar{q}q$  substructure. This is most marked for the pion and enters the pion loop integral in Eq. (39) through the factors  $Z_\pi^{-1}(q_\pm^2)$  which are contributed by each pion propagator. (In our calculational procedure these factors have been moved into the vertex functions for convenience.) If each function  $Z_\pi$  is held constant at its mass-shell value (as would be the case for a structureless pion), the full calculation

in Fig. 7 (solid line) becomes the dot-dashed line. The intercept then indicates that the mass shift would be essentially zero. In contrast to this, the short dashed line indicates that the influence of the corresponding quantity  $Z_1(P^2)$ , from the substructure of the  $\rho$ , is quite negligible here. This is because the range of variation in  $P^2$  is very small.

In a parallel manner, the pion loop contribution to the transverse  $\rho^0$ – $\omega$  mixing amplitude is calculated from

$$\Pi^\pi(P^2) = -\frac{4}{3}f_{\rho\pi\pi}(P^2)f_{\omega\pi\pi}(P^2) \int \frac{d^4q}{(2\pi)^4} \frac{(q^2 - (q \cdot P)^2/P^2)e^{-q^2/\lambda^2(P^2)}}{\left[(q + \frac{P}{2})^2 + m_\pi^2 - i\epsilon\right] \left[(q - \frac{P}{2})^2 + m_\pi^2 - i\epsilon\right]} \quad (49)$$

where  $\lambda^{-2} = \lambda_\rho^{-2} + \lambda_\omega^{-2}$ . The results are shown in Fig. 8. An experimental value [22] for the total real mixing amplitude is also displayed. The pion loop mechanism produces a significantly smaller real amplitude than does the quark-loop mechanism and does not have a node near zero momentum. In Fig. 9 we illustrate the contributions to  $\text{Re } \Pi^\pi$  made by the dynamical nature of the meson self-energy functions. When the pion quantities  $Z_\pi(q_\pm^2)$  are held fixed at the mass-shell value, the full calculation (solid line) reduces to the dot-dashed line. As with the  $\rho$  self-energy, the dynamical  $\bar{q}q$  substructure of the pion has a considerable influence on the pion loop mixing mechanism near the vector meson mass-shell. The difference between the solid and dashed lines shows that the corresponding vector meson substructure plays a lesser role. We compare the quark loop (dashed line) and pion loop (dotted line) contributions to the real mixing amplitude in Fig. 10. The solid line is the sum of the two. At the mass-shell, the quark loop dominates with the pion-loop contributing about 20% of the total. For spacelike momenta, the pion loop contribution is negligible.

The change of basis associated with the diagonal form of the inverse propagator given in Eq. (42) produces physical fields given by

$$\begin{pmatrix} \rho \\ \omega \end{pmatrix} = \begin{pmatrix} 1 & -\epsilon \\ \epsilon & 1 \end{pmatrix} \begin{pmatrix} \rho_I \\ \omega_I \end{pmatrix}. \quad (50)$$

Currents that couple to  $\rho_I$  and  $\omega_I$  are mixed in the same way. Thus the resonant  $\rho$  and  $\omega$  contribution to the time-like pion charge form factor is given by

$$F_\pi^R(P^2) = F_{\omega\pi\pi}(P^2)\mathcal{D}_\omega(P^2)f_{\omega\gamma}(P^2) + F_{\rho\pi\pi}(P^2)\mathcal{D}_\rho(P^2)f_{\rho\gamma}(P^2), \quad (51)$$

where  $\mathcal{D}_\omega(P^2) = [P^2 + m_\omega^2]^{-1}$  and  $\mathcal{D}_\rho(P^2) = [P^2 + m_\rho^2 - im_\rho\Gamma(P^2)]^{-1}$ . The  $2\pi$  form factors of the physical vector mesons are

$$F_{\omega\pi\pi}(P^2) = F_{\omega_I\pi\pi}(P^2) + \epsilon(P^2)F_{\rho_I\pi\pi}(P^2) \\ F_{\rho\pi\pi}(P^2) = \frac{1}{\sqrt{Z_2(P^2)}} \left( F_{\rho_I\pi\pi}(P^2) - \epsilon(P^2)F_{\omega_I\pi\pi}(P^2) \right). \quad (52)$$

The form factors in the isospin basis have been described in Sec. V. The dependence of the electromagnetic coupling strengths  $f_{\rho\gamma}$  and  $f_{\omega\gamma}$  on the mixing amplitude must be accounted for in a fit to data. (See, for example Ref. [23].) Here we limit our consideration to aspects of the  $2\pi$  decay. Since the mixing amplitude  $\epsilon$  is part of a small second order effect in  $F_{\rho\pi\pi}(P^2)$ , it is the resonant  $\omega$  contribution, and in particular the physical coupling constant

$g_{\omega\pi\pi} = F_{\omega\pi\pi}(-m_\omega^2)$ , which carries the leading information on the mixing amplitude. From Eq. (52) we may write

$$g_{\omega\pi\pi} = g_{\omega_I\pi\pi} + \epsilon(-m_\omega^2) F_{\rho_I\pi\pi}(-m_\omega^2), \quad (53)$$

by making use of the fact that  $\omega$  and  $\omega_I$  have the same mass at the present level of approximation. Given that  $F_{\rho_I\pi\pi}(-m_\omega^2)$  is well determined by the known  $g_{\rho\pi\pi}$ , knowledge of  $g_{\omega_I\pi\pi}$  is necessary before  $\epsilon$  can be deduced from a value of  $g_{\omega\pi\pi}$  extracted from data analysis.

For the calculated total mixing amplitude at the  $\omega$  mass shell, we find  $\Pi^{\rho\omega}(-m_\omega^2) = -(2.6 + 2.3i) \times 10^{-3} \text{ GeV}^2$ . The real part is substantially below the experimental value [22] of  $-(4.52 \pm 0.6) \times 10^{-3} \text{ GeV}^2$  from analysis of the  $e^+e^- \rightarrow \pi^+\pi^-$  data. This latter value relies upon assumptions [21] in the analysis that lead to the cancellation of the direct  $\omega_I \rightarrow \pi\pi$  mechanism with  $\text{Im } \Pi^{\rho\omega}$ . A recent re-analysis [23] has pointed out that the corrections to these assumptions lead to an increase of about a factor of three in the uncertainty of the extracted real mixing amplitude in the absence of theoretical limits on  $g_{\omega_I\pi\pi}$ . Our result for  $\text{Re } \Pi^{\rho\omega}(-m_\omega^2)$  is just within such an allowed range. The pion loop contribution to the  $\rho$  self-energy is found to be  $\Pi^{\rho\rho}(-m_\omega^2) = -(0.31 + 1.1i) \times 10^{-1} \text{ GeV}^2$  giving a mixing parameter  $|\epsilon(-m_\omega^2)| = 0.0303$ ,  $\arg(\epsilon) = 147.2^\circ$  from Eq. (41).

The influence of the direct coupling term  $g_{\omega_I\pi\pi}$  within the present model can be assessed as follows. With Eq. (41) for  $\epsilon$ , Eq. (53) becomes

$$g_{\omega\pi\pi} = -\frac{\text{Re } \Pi^{\rho\omega}}{\Pi^{\rho\rho}} g_{\rho_I\pi\pi} + \frac{g_{\omega_I\pi\pi} \Pi^{\rho\rho} - i \text{Im } \Pi^{\rho\omega} g_{\rho_I\pi\pi}}{\Pi^{\rho\rho}}, \quad (54)$$

where we write  $F_{\rho_I\pi\pi}(-m_\omega^2) \approx g_{\rho_I\pi\pi}$  since the shifted mass-shell point is a minor correction to this quantity. Although the amplitudes  $\Pi^{\rho\omega}(P^2)$  and  $\Pi^{\rho\rho}(P^2)$  here are to be evaluated at  $-m_\omega^2$ , the arguments below are not altered significantly by changes in the mass-shell point compatible with the  $\rho - \omega$  mass difference. The second term above is usually eliminated by making two assumptions [21]. Firstly,  $\text{Re } \Pi^{\rho\rho}$  is taken to be zero. Apart from small adjustments due to the momentum dependence, this ignores the  $\rho - \omega$  mass difference given in Eq. (43). Secondly,  $\text{Im } \Pi^{\rho\omega}$  is assumed to be  $\text{Im } \Pi^{\rho\rho}$  scaled down by  $g_{\omega_I\pi\pi}/g_{\rho_I\pi\pi}$ . This would be exact in the present model if the  $\rho\pi\pi$  and  $\omega\pi\pi$  form factors were characterized by the same momentum dependent shape. As we have seen from Figs. 4 and 5, this is only true in a qualitative sense. As a result of the relevant loop integrals for the self-energies, there is an approximate scaling behavior evident in Figs. 6 and 8. Quantitatively, we find this second assumption to be in error by about 17% at the mass shell. To assess the net effect of these approximations, Eq. (54) may be expressed as

$$g_{\omega\pi\pi} = -\frac{(\text{Re } \Pi^{\rho\omega}) \mathcal{C}}{i \text{Im } \Pi^{\rho\rho}} g_{\rho_I\pi\pi} \quad (55)$$

where the denominator is determined by the  $\rho$  mass and width via Eq. (46). The departure of the correction factor  $\mathcal{C}$  from its conventional value of unity is a measure of the accuracy of the approximations mentioned above. Within the present model we find  $|\mathcal{C}| = 0.78$  and  $\arg(\mathcal{C}) = 25^\circ$ . A significant part of this correction is generated by  $g_{\omega_I\pi\pi} \text{Re } \Pi^{\rho\rho}$  and thus is a measure of the competing influence of the usually neglected direct  $\omega_I \rightarrow \pi\pi$  process. The trend is for a deduced value of  $\text{Re } \Pi^{\rho\omega}$  to be some 20% larger than what would otherwise be needed for the same  $g_{\omega\pi\pi}$ .

## VII. DISCUSSION

In this work, we have found that a number of properties of the  $\rho - \omega$  system can be described by a phenomenological treatment of dressed quark degrees of freedom as implemented by an effective field theory model applied up to one pion loop. A distinguishing feature of the present approach is that the finite size  $\bar{q}q$  substructure of the mesons is included. This substructure for the pion is correlated with the momentum-dependent scalar self-energy dressing of the quark through chiral symmetry considerations. The resulting dynamical nature of the mass function in the pion propagator is included in the calculated pion loop contributions to both the mixed  $\rho^0 - \omega$  self-energy and the diagonal self-energy in the  $\rho$  channel. The latter produces a reasonable value for the  $\rho - \omega$  mass difference if the influence of the  $\bar{q}q$  substructure effects on the pion propagator are included. If we use the point particle limit of the pion propagator, this mass difference becomes negligible. The total  $\rho^0 - \omega$  mixing here consists of a quark loop and a pion loop part and the latter is found to contribute 20% at the mass-shell. For spacelike momenta appropriate to mixed  $\rho - \omega$  exchange for the NN force, the pion loop mixing contribution is not significant and the total mixing amplitude remains much too small to explain the empirical CSB NN force.

The calculated values of  $g_{\rho\pi\pi}$  and  $m_\omega$  are used to fix two parameters that we have introduced to minimally add the vector mesons to a previously developed parameterization of pion physics that is the basis of the quark-level approach we employ. The isospin breaking quantities calculated here, i.e. the  $\rho^0 - \omega$  mixing amplitude and the coupling constant  $g_{\omega I\pi\pi}$ , scale in an approximately linear way with the quark bare mass difference and we have presented our results for the typical value  $\delta m = -4$  MeV.

We do not consider the contribution of  $\rho^0 - \omega$  mixing to the meson masses because it is an effect of second order in the mixing amplitude. For a similar reason we do not consider the one pion loop correction to  $m_\omega$ . In our pion loop calculations, we have used the empirical value of  $g_{\rho\pi\pi}$  to set the strength of the  $\rho_I^0\pi\pi$  vertex even though the empirical coupling constant refers to the physical  $\rho^0$  which is a linear combination of  $\rho_I^0$  and  $\omega_I$ . For a calculation that is strictly of lowest order in the mixing amplitude, one should use the model results for the mixing to deduce a value for  $g_{\rho I\pi\pi}$  and iterate the calculation until there is self-consistency. However consideration of Eq. (52) shows that the correction is a small second order effect and we do not make it.

In this work the coupling constant  $g_{\omega I\pi\pi}$  is found to be  $g_{\omega I\pi\pi} = 0.105$ . We examine the correction that this direct process brings to the relation between the  $\omega \rightarrow \pi\pi$  decay and  $\rho^0 - \omega$  mixing amplitude. The trend is for the necessary real mixing amplitude to be some 20% larger than what would otherwise be the case. There is also a phase consequence and specific details can be found in Eq. (55).

In a future work some of the approximations we make could be removed and some reduction could be sought in the degree of phenomenology employed. Although the strength of the single scalar function we use for the vector meson BS amplitude is determined by the mass-shell normalization internal to the model, the range of the gaussian form is described by a free parameter constrained by the calculated  $g_{\rho\pi\pi}$ . We believe the result to be physically sensible because, in this same general framework, it leads to the prediction [7,8]  $g_{\gamma\pi\rho} = 0.50$  which is to be compared to  $g_{\gamma\pi\rho}^{expt} = 0.504$ . Nevertheless, it is of interest to check these results with a vector meson amplitude that solves a BS equation and allows more than just the



canonical Dirac matrix covariant. Such numerical solutions are available [26]. However it is difficult to accommodate the consequences of the complex values of quark loop momenta produced by mass-shell values of meson momenta in the Euclidean metric of this model. An ansatz for treatment of the ladder BS equation developed in recent works [27,37] goes a long way to overcoming this obstacle. Those works provide conveniently expressed BS amplitudes with parameters set by pion and kaon properties. One such approach [27] allows a number of independent covariants selected by the dynamics and the predicted amplitudes for  $\rho$  and  $\omega$  do confirm that the single canonical covariant used in the present work is strongly dominant. The other approach [37] also provides a convenient form of the bare mass dependence of parameterized quark propagators that is somewhat more general than what we consider here and it would be of interest to explore the consequences.

## ACKNOWLEDGMENTS

This work was supported in part by the National Science Foundation under Grant Nos. PHY91-13117 and PHY94-14291. We wish to thank K. Maltman for several very helpful discussions.

## APPENDIX: MESONS FROM QUARKS

Hadronization of the quark action of Eq. (1) can be implemented through a functional change of field variables in the path integral for the generating functional. The meson sector follows directly from a standard Fierz reordering of the current-current term of the action in Eq. (1) to obtain

$$\frac{1}{2}j_\mu^a(x)D(x-y)j_\mu^a(y) = -\frac{1}{2}J^\theta(x,y)D(x-y)J^\theta(y,x), \quad (\text{A1})$$

in terms of bilocal currents  $J^\theta(x,y) = \bar{q}(x)\Lambda^\theta q(y)$ . The  $\Lambda^\theta$  are direct products of Dirac spin,  $SU(2)$  flavor, and  $SU(3)$  color matrices, viz.

$$\Lambda^\theta = \frac{1}{2} \left( \mathbf{1}_D, i\gamma_5, \frac{i}{\sqrt{2}}\gamma_\nu, \frac{i}{\sqrt{2}}\gamma_\nu\gamma_5 \right) \otimes \left( \frac{\mathbf{1}_F}{\sqrt{2}}, \frac{\tau^a}{\sqrt{2}} \right) \otimes \left( \frac{4}{3}\mathbf{1}_C, \frac{i}{\sqrt{3}}\lambda^a \right). \quad (\text{A2})$$

We are here interested in the color singlet  $\bar{q}q$  sector. There is however, a color octet  $\bar{q}q$  sector in Eq. (A2). An alternate color Fierz reordering may be used to eliminate the color octet  $\bar{q}q$  sector in favor of color anti-triplet  $qq$  and  $\bar{q}\bar{q}$  pairings which find a natural role as constituents of baryons [25]. However only the color singlet meson modes from Eq. (A2) are of concern here. The part of the integrand of the partition function  $Z = N \int D\bar{q}Dq \exp(-S[\bar{q},q])$  that arises from the right side of Eq. (A1) may be expressed as the integral

$$\exp\left(\frac{1}{2}(J, DJ)\right) = N' \int D\mathcal{B} \exp\left[-\frac{1}{2}(\mathcal{B}, D^{-1}\mathcal{B}) - (J, \mathcal{B})\right] \quad (\text{A3})$$

where the bracket notation denotes the relevant space-time integration and summation over internal degrees of freedom. The net result is the reformulation  $Z = N'' \int D\mathcal{B} D\bar{q}Dq$

$\exp(-S[\bar{q}, q, \mathcal{B}])$  where the new action has no four fermion term but instead contains  $(J, \mathcal{B}) \equiv \int d^4x, y \bar{q}(x) \Lambda^\theta \mathcal{B}^\theta(x, y) q(y)$ , a linear coupling of an appropriate set of bilocal auxiliary fields  $\mathcal{B}^\theta$  to quarks. To preserve the symmetries of the original action, it is necessary that the fields  $\mathcal{B}^\theta(x, y)$  have the same transformation properties as the currents  $\bar{q}(y) \Lambda^\theta q(x)$ . These auxiliary fields are then bosons that take on the dynamics of  $\bar{q}q$  correlations. For example, the  $\omega$  meson of the model will be dominated by the component associated with  $\Lambda^\theta \propto i\gamma_\mu$ . With the action now quadratic in the quark fields, they may be integrated out by standard methods. The partition function then has the representation  $Z = \mathcal{N} \int D\mathcal{B} e^{-S[\mathcal{B}]}$  in terms of a bosonized action given by

$$S[\mathcal{B}] = -\text{TrLn} [\not{\partial} + m + \Lambda^\theta \mathcal{B}^\theta] + \int d^4x d^4y \frac{\mathcal{B}^\theta(x, y) \mathcal{B}^\theta(y, x)}{2D(x - y)}. \quad (\text{A4})$$

An effective action for the propagating meson modes is defined by expansion in fluctuations about the saddle point of the action (which is equivalent to the classical vacuum). From  $\delta S[\mathcal{B}_0]/\delta \mathcal{B}_0 = 0$ , these classical configurations given by  $\mathcal{B}_0^\theta(r) = D(r) \text{tr}[\Lambda^\theta (\not{\partial} + m + \Lambda^\theta \mathcal{B}_0^\theta(r))^{-1}]$  are related to nonlocal vacuum condensates and provide a quark self-energy  $\Sigma(r) = \Lambda^\theta \mathcal{B}_0^\theta(r)$ . This is equivalent to the ladder Dyson-Schwinger equation in the bare vertex or rainbow approximation

$$\Sigma(p) = \int \frac{d^4q}{(2\pi)^4} D(p - q) \frac{\lambda^a}{2} \gamma_\mu \frac{1}{i\gamma \cdot q + m + \Sigma(q)} \frac{\lambda^a}{2} \gamma_\mu. \quad (\text{A5})$$

From the general form  $\Sigma(p) = i \not{p} [A(p^2) - 1] + B(p^2)$ , the dressed quarks now have a dynamically-generated mass function  $M(p^2) = (B(p^2) + m)/A(p^2)$  and become the constituents of the meson modes.

The meson modes are defined by expansion of the action about the saddle point configuration of each auxiliary field. That is, one sets

$$\Lambda^\theta \mathcal{B}^\theta(x, y) = \Sigma(x - y) + i\gamma_5 \vec{\tau} \cdot \vec{\pi}(x, y) + i\gamma_\mu \omega_\mu(x, y) + \cdots, \quad (\text{A6})$$

where  $\vec{\pi}(x, y) + \cdots$  are the new field variables, to produce the meson action from

$$\hat{S}[\pi, \rho, \omega \cdots] = S[\mathcal{B}] - S[\mathcal{B}_0]. \quad (\text{A7})$$

This will consist of terms at the quadratic and higher order level in the meson fields. Contact with effective local field variables may be made in the following way [38]. For each fluctuation field  $\phi$ , the free inverse propagator is given by  $\mathcal{D}^{-1} = \delta^2 \hat{S}/\delta \phi^2$  at  $\phi = 0$ . The free equation of motion  $\mathcal{D}^{-1} \hat{\Gamma} = 0$  produces the ladder Bethe-Salpeter equation for the amplitude  $\hat{\Gamma}$ . The set of eigenfunctions produced by  $\mathcal{D}^{-1} \hat{\Gamma}_n = \alpha_n \hat{\Gamma}_n$  may be used to expand the bilocal fluctuation fields thereby discretizing the continuous internal degree of freedom in terms of known amplitudes, leaving a local field as the remaining variable. Thus, for example, one arrives at the representation  $\pi(q; P) = \sum_n \hat{\Gamma}_n(q; P) \pi_n(P)$  where  $q$  is the internal momentum conjugate to  $x - y$ , and  $P$ , conjugate to  $(x + y)/2$ , is the total momentum of the meson mode described by the local variable  $\pi_n$ . With truncation to the lowest mass mode in each case, the result is Eq. (2).

## REFERENCES

- \* Present Address: TRIUMF, 4004 Wesbrook Mall, Vancouver, British Columbia, Canada V6T 2A3.
- [1] C. D. Roberts, in *Chiral Dynamics: Theory and Experiment*, A. M. Bernstein and B. R. Holstein (Eds.), Lecture Notes in Physics, **452**, p. 68 (Springer, Berlin 1995); C. D. Roberts, *Electromagnetic Pion Form Factor and Neutral Pion Decay Width*, ANL preprint # ANL-PHY-7842-TH-94 (1994), Nucl. Phys. **A**, in press.
  - [2] C.J. Burden, C.D. Roberts and M.J. Thomson, Phys. Lett. **B371**, 163 (1996).
  - [3] C. D. Roberts and A. G. Williams, Prog. Part. Nucl. Phys. **33**, 477 (1994).
  - [4] C.D. Roberts, R.T. Cahill, M.E. Sevier and N. Iannella, Phys. Rev. **D49**, 125 (1994).
  - [5] M. R. Frank, K. L. Mitchell, C. D. Roberts and P. C. Tandy, Phys. Lett. B **359**, 17 (1995).
  - [6] R. Alkofer and C. D. Roberts, Phys. Lett. B **369**, 101 (1996).
  - [7] K. L. Mitchell, Ph.D. Thesis, Kent State University, unpublished 1995.
  - [8] P. C. Tandy, Prog. Part. Nucl. Phys. **36**, 97 (1996).
  - [9] K. L. Mitchell, P. C. Tandy, C. D. Roberts and R. T. Cahill, Phys. Lett. **B335**, 282 (1994).
  - [10] R. T. Cahill and C. D. Roberts, Phys. Rev. **D32**, 2419 (1985).
  - [11] J. Praschifka, C. D. Roberts, and R. T. Cahill, Phys. Rev. **D36**, 209 (1987).
  - [12] Y. Nambu and G. Jona-Lasinio, Phys. Rev. **122**, 345 (1961); U. Vogel and W. Weise, Prog. Part. Nucl. Phys. **27**, 195 (1991).
  - [13] R. Friedrich and H. Reinhardt, Nucl. Phys. **A594**, 406 (1995).
  - [14] Shun-fu Gao, C. M. Shakin and Wei-Dong Sun, Phys. Rev. **C53**, 1374 (1996).
  - [15] C. M. Shakin and Wei-Dong Sun, *Direct  $\omega \rightarrow \pi^+ \pi^-$  decay in the analysis of rho-omega mixing*, preprint BCCNT 96/031/254, March 1996.
  - [16] T. Goldman, J. A. Henderson and A. W. Thomas, Few-Body Sys. **12**, 123 (1992).
  - [17] G. Krein, A. W. Thomas and A. G. Williams, Phys. Lett. **B317**, 293 (1993).
  - [18] S. Gardner, C. J. Horowitz and J. Piekarewicz, Phys. Rev. Lett. **75**, 2462 (1995); Phys. Rev. **C53**, 1143 (1996).
  - [19] C.D. Roberts, R.T. Cahill and J. Praschifka, Int. J. Mod. Phys. **A4**, 719 (1989); L. C. L. Hollenburg, C. D. Roberts and B. H. J. McKellar, Phys. Rev. **C46**, 2057 (1992).
  - [20] J. Praschifka, C.D. Roberts and R.T. Cahill, Int. J. Mod. Phys. **A2**, 1797 (1987).
  - [21] F. M. Renard, in Springer Tracts in Modern Physics, **63**, 98 (Springer-Verlag, 1972).
  - [22] P. C. McNamee, M. D. Scadron and S. A. Coon, Nucl. Phys. **A249**, 483 (1975); S. A. Coon and R. G. Barrett, Phys. Rev. **C36**, 2189 (1987).
  - [23] K. Maltman, H. B. O'Connell and A. G. Williams, Phys. Lett. **B376**, 19 (1996).
  - [24] K. Maltman, Phys. Rev. **D53**, 2563 (1996).
  - [25] R. T. Cahill, Nucl. Phys. **A543**, 63c (1992).
  - [26] P. Jain and H. Munczek, Phys. Rev. **D48**, 5403 (1993).
  - [27] C.J. Burden, Lu Qian, C.D. Roberts, P.C. Tandy and M.J. Thomson, *Ground State Spectrum of Light-quark Mesons*, submitted to Phys. Rev. **C**, May 1996; preprint ANL-PHY-8421-TH-96 and KSUCNR-03-96.
  - [28] R. Delbourgo and M. D. Scadron, J. Phys. **G5**, 1631 (1979).
  - [29] M. R. Frank and C.D. Roberts, Phys. Rev. **C53**, 390 (1996).
  - [30] M. Gell-Mann, R. Oakes and B. Renner, Phys. Rev. **175**, 2195 (1968).

- [31] R. T. Cahill and S. M. Gunner, Mod. Phys. Lett. **A10**, 3051 (1995).
- [32] C. Itzykson and J. R. Zuber, *Quantum Field Theory*, McGraw-Hill, New York, 1980, pp. 481-485.
- [33] C. D. Roberts, A. G. Williams and G. Krein, Int. J. Mod. Phys. **A7**, 5607 (1992).
- [34] C. J. Burden, C. D. Roberts and A. G. Williams, Phys. Lett. **B285**, 347 (1992).
- [35] A. G. Williams, G. Krein and C. D. Roberts, Ann. Phys. (NY) **210**, 464 (1991).
- [36] H. B. O'Connell, B. C. Pearce, A. W. Thomas and A. G. Williams, in *Trends in Particle and Nuclear Physics*, ed. W. Y. P. Hwang (Plenum. 1996).
- [37] R. T. Cahill and S. M. Gunner, Phys. Lett. **B359**, 281 (1995).
- [38] R. T. Cahill, Aust. J. Phys. **42**, 171 (1989).

# FIGURES

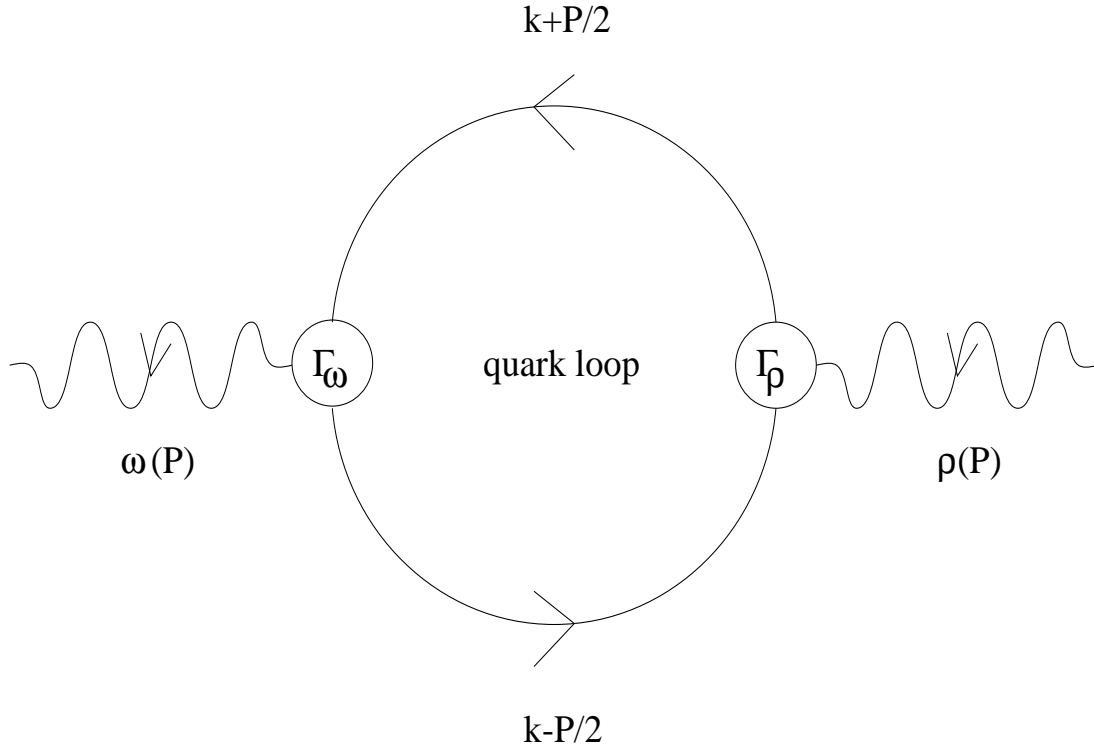


FIG. 1. The quark-loop mechanism for  $\rho\omega$  mixing.

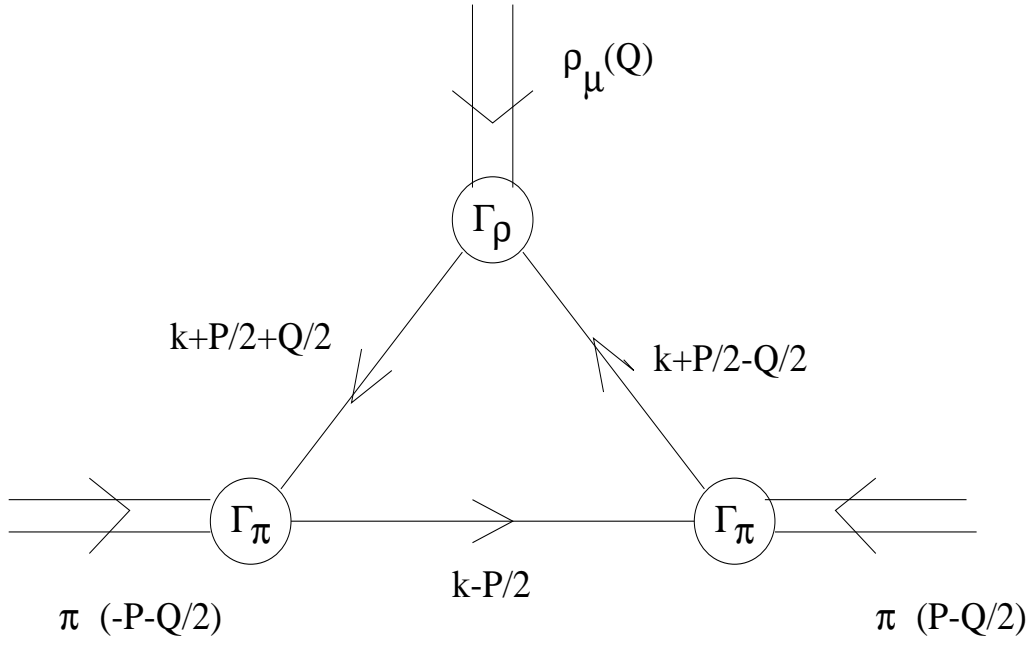


FIG. 2. The quark loop mechanism for  $\rho\pi\pi$  coupling.

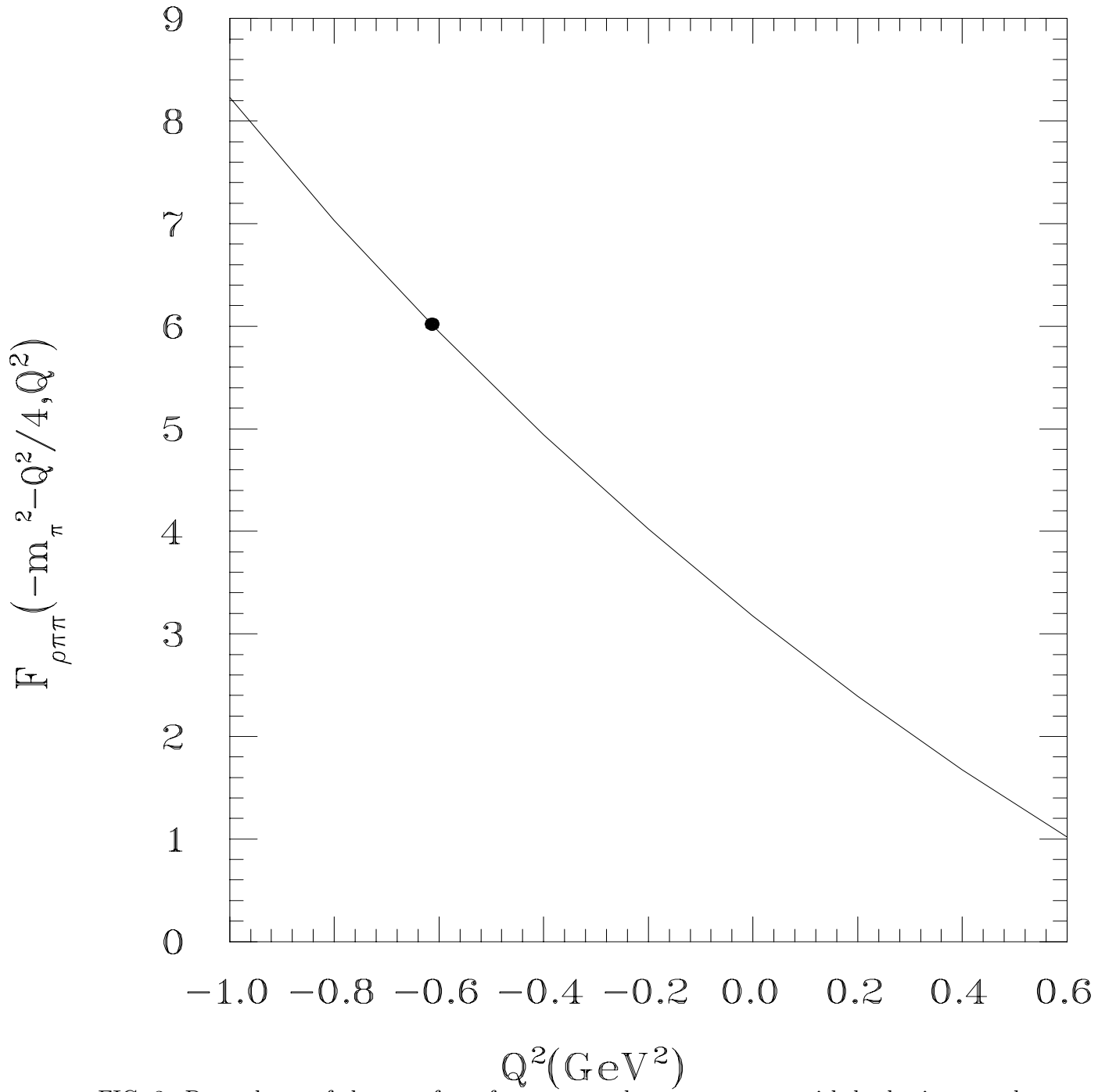


FIG. 3. Dependence of the  $\rho\pi\pi$  form factor upon the  $\rho$  momentum with both pions on the mass-shell. The dot represents the  $\rho$  mass-shell.

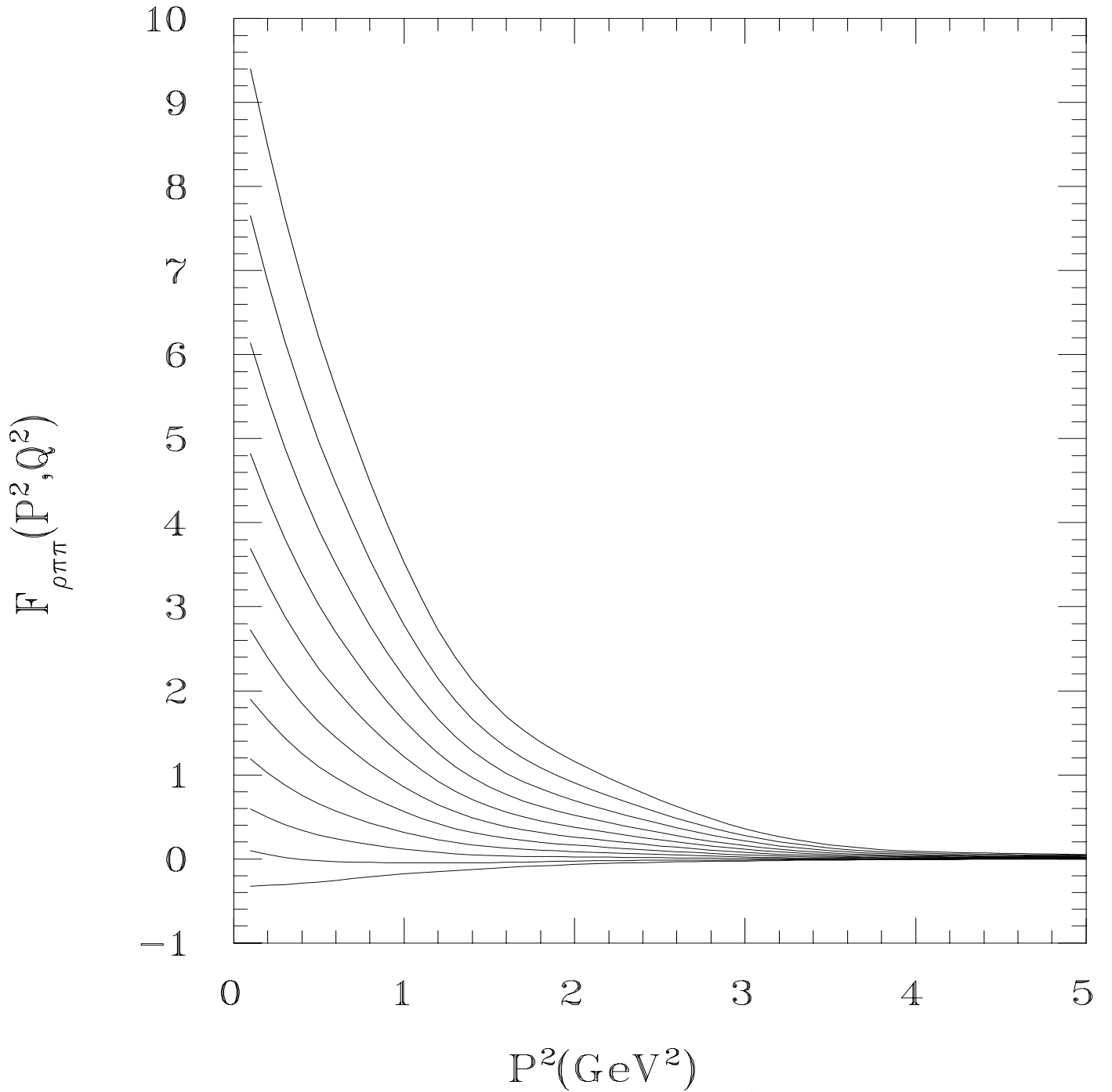


FIG. 4. The  $\rho\pi\pi$  form factor. The top curve is for  $Q^2 = -1 \text{ GeV}^2$  and the bottom curve is for  $Q^2 = 1 \text{ GeV}^2$ . Equal increments of  $\Delta Q^2 = 0.2 \text{ GeV}^2$  are used in between.



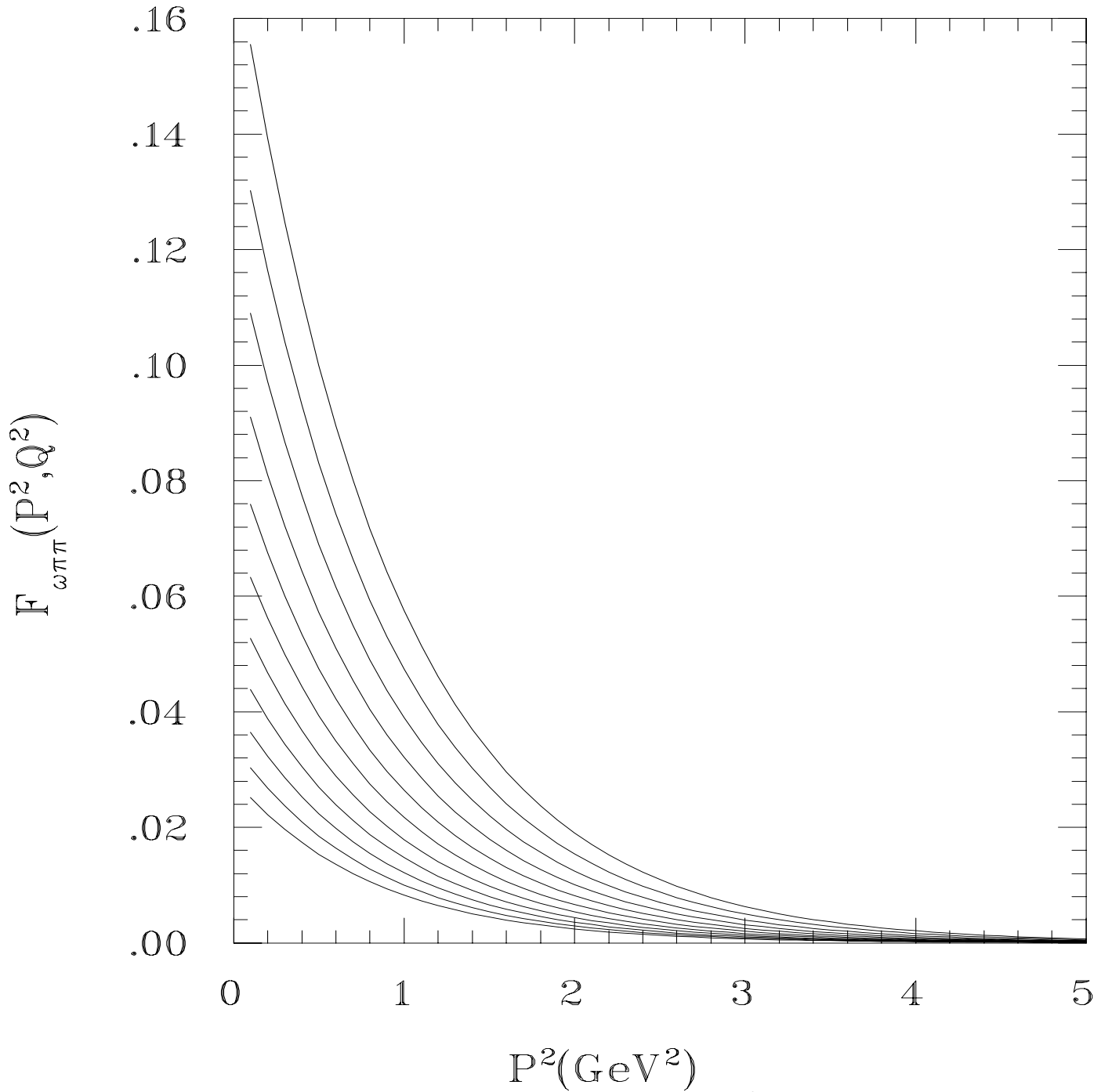


FIG. 5. The  $\omega\pi\pi$  form factor. The top curve is for  $Q^2 = -1 \text{ GeV}^2$  and the bottom curve is for  $Q^2 = 1 \text{ GeV}^2$ . Equal increments of  $\Delta Q^2 = 0.2 \text{ GeV}^2$  are used in between.

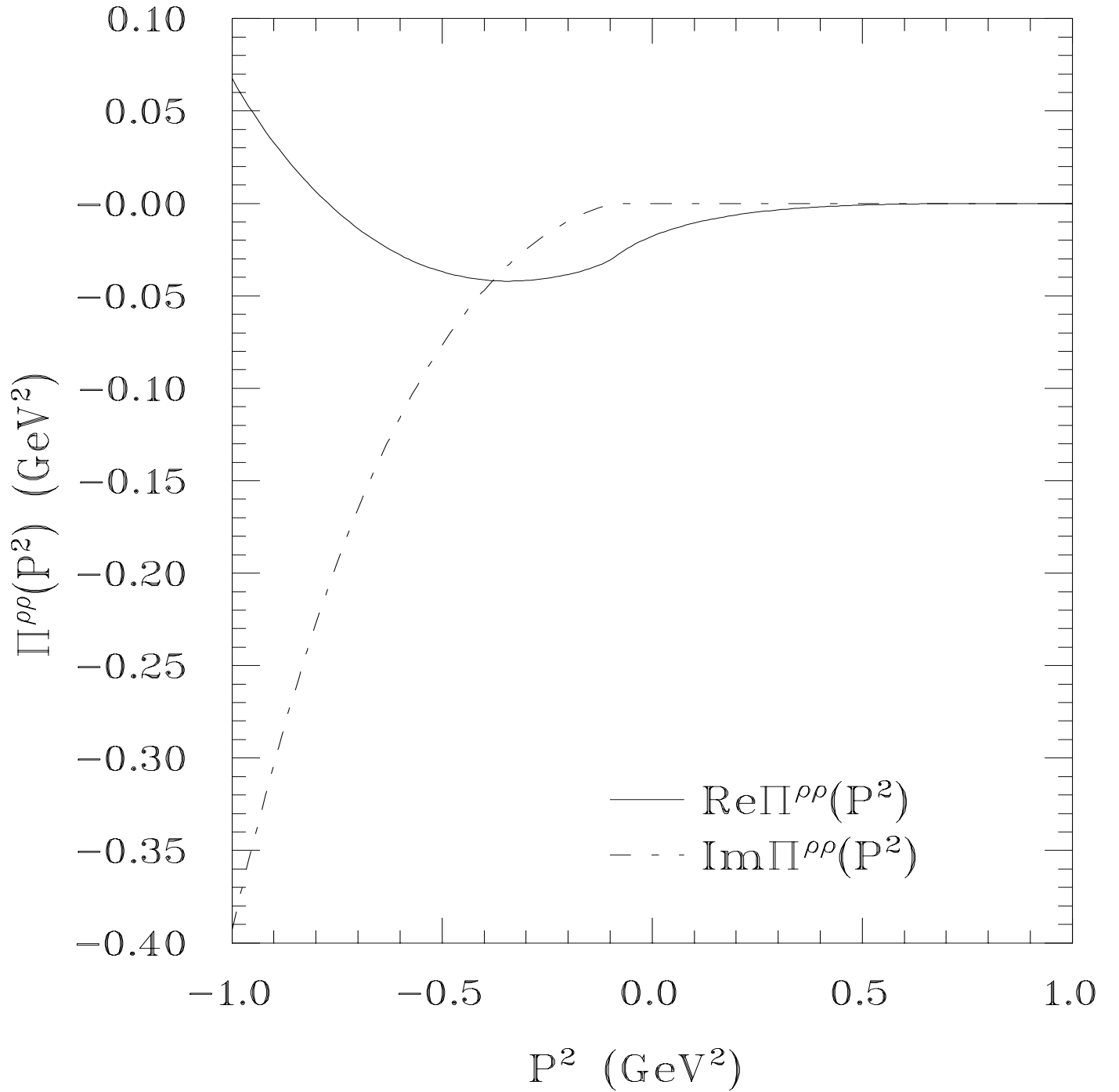


FIG. 6. The real and imaginary parts of the pion loop contribution to the  $\rho$  self-energy.

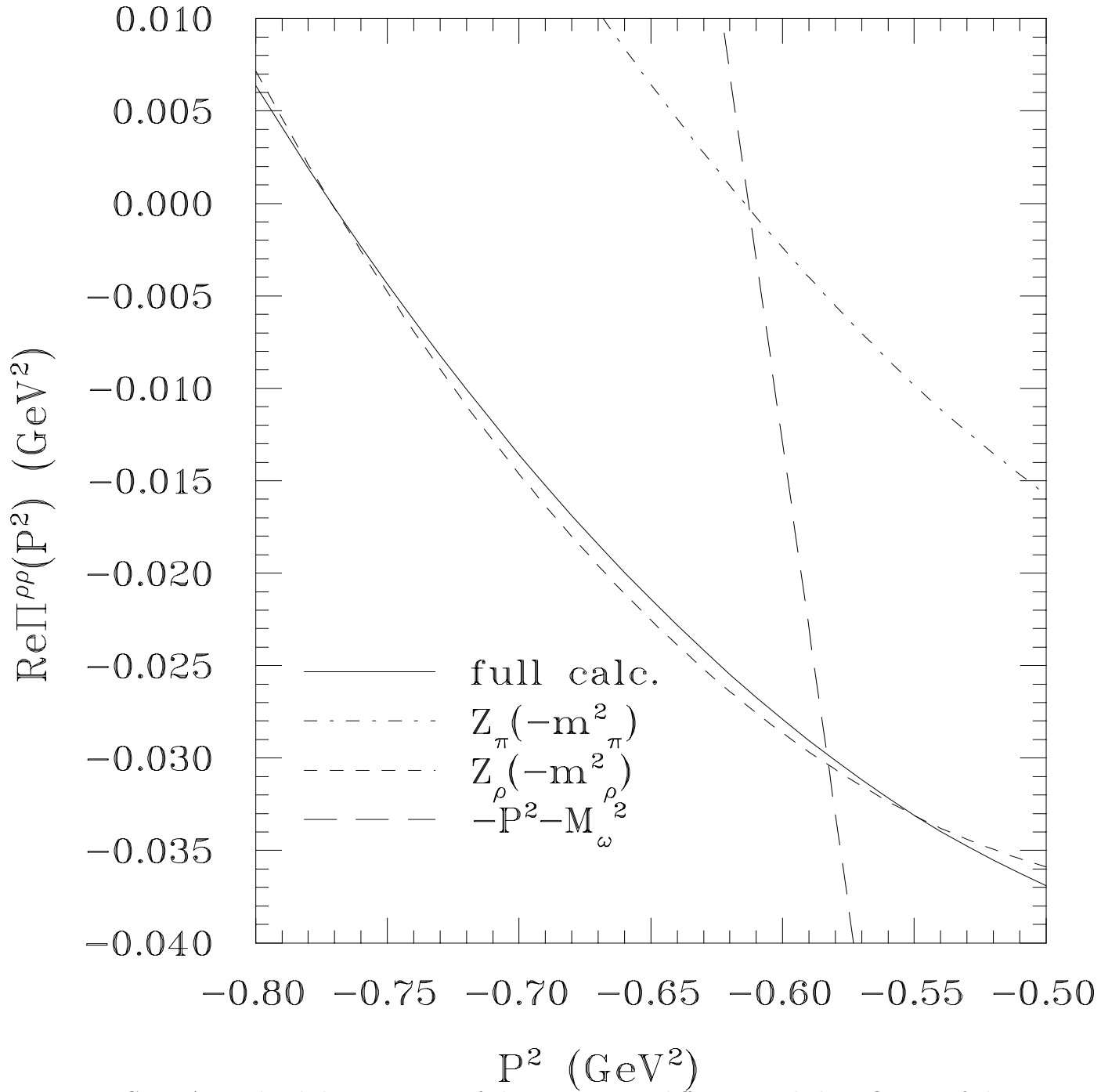


FIG. 7. A graphical determination of the  $\rho - \omega$  mass difference and the influence of the  $\bar{q}q$  composite nature of the  $\pi$  and  $\rho$  propagators as described in the text.

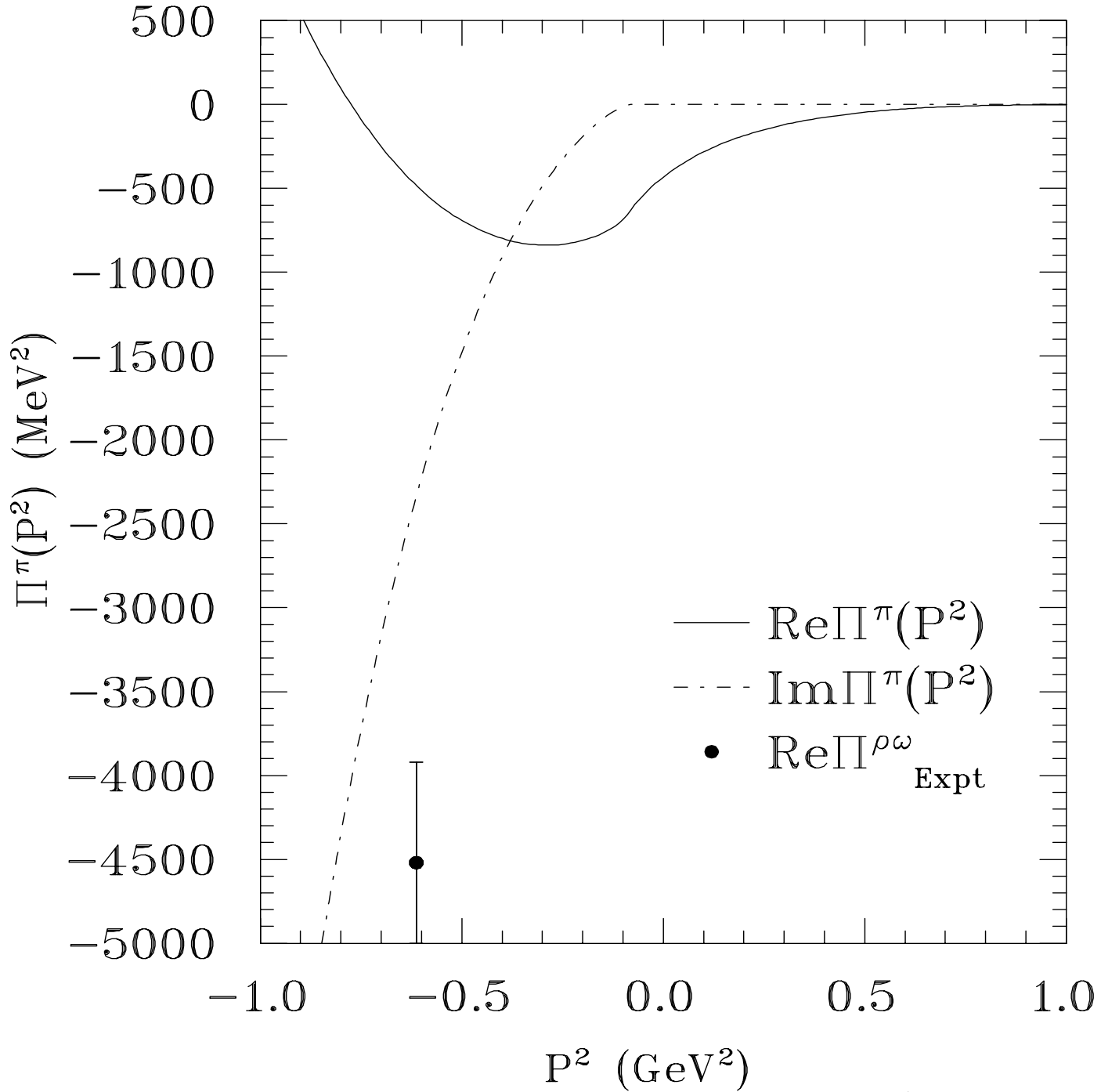


FIG. 8. The real and imaginary parts of the pion loop contribution to the  $\rho^0 - \omega$  mixing amplitude.

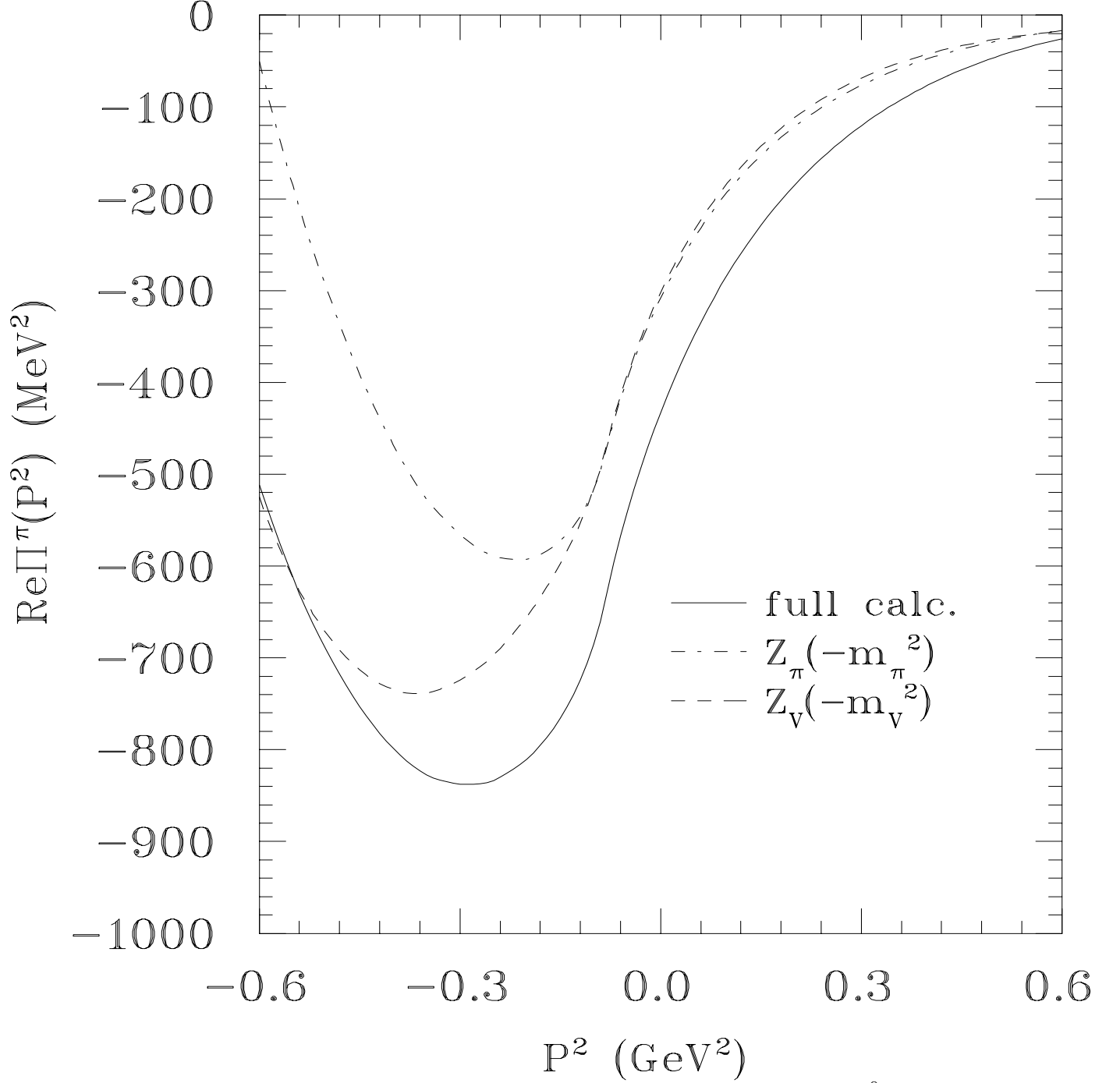


FIG. 9. Various  $\bar{q}q$  substructure effects on the pion loop contribution to  $\rho^0 - \omega$  mixing as described in the text.

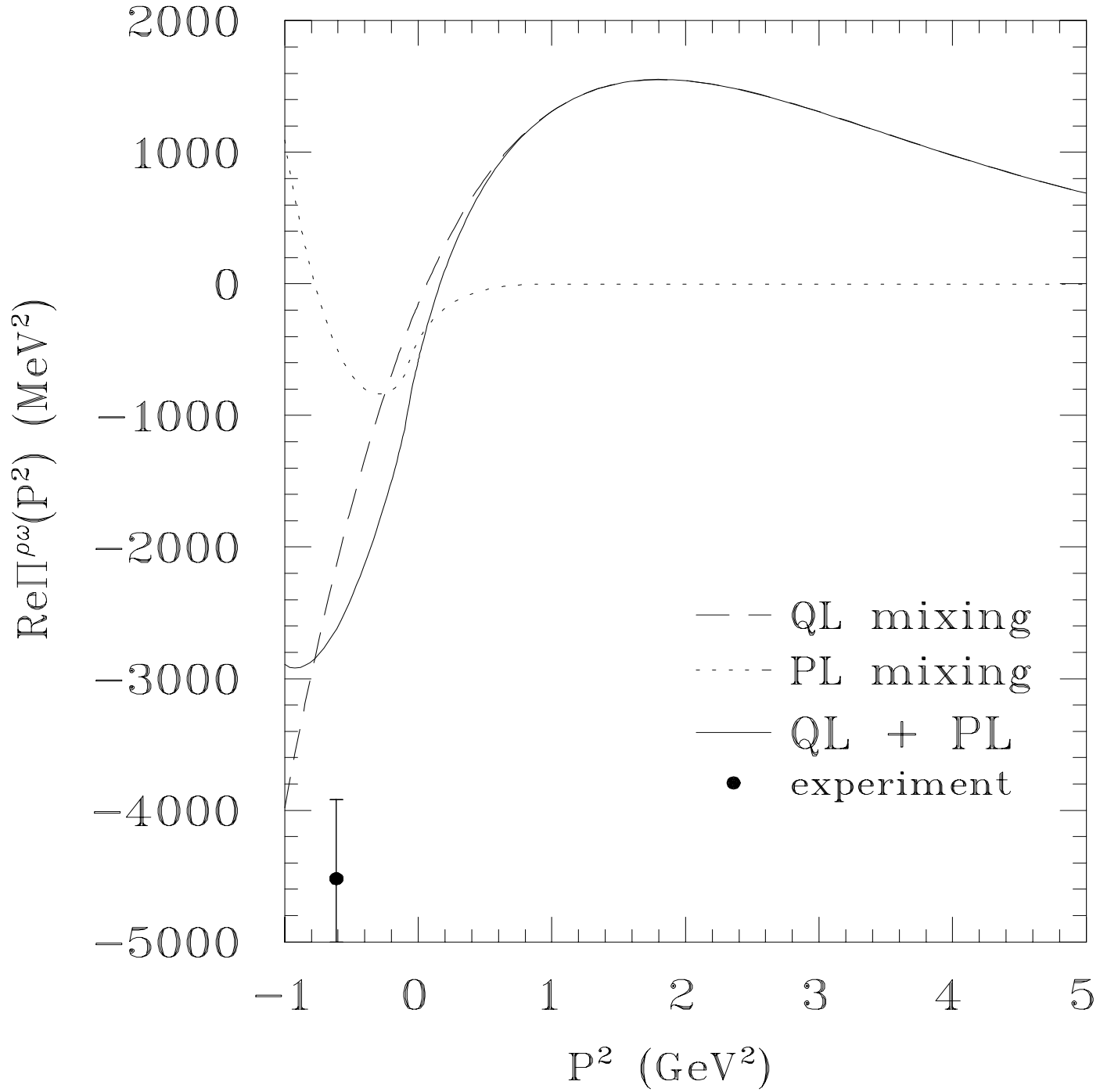


FIG. 10. The quark loop (QL) and pion loop (PL) contributions to the  $\rho^0 - \omega$  mixing amplitude.